

# Tradeoffs between convergence rate and noise amplification for momentum-based accelerated optimization algorithms

Hesameddin Mohammadi, Meisam Razaviyayn, and Mihailo R. Jovanović

## Abstract

We study momentum-based first-order optimization algorithms in which the iterations utilize information from the two previous steps and are subject to an additive white noise. This class of algorithms includes Polyak’s heavy-ball and Nesterov’s accelerated methods as special cases and noise accounts for uncertainty in either gradient evaluation or iteration updates. For strongly convex quadratic problems, we use the steady-state variance of the error in the optimization variable to quantify noise amplification and identify fundamental stochastic performance tradeoffs. Our approach utilizes the Jury stability criterion to provide a novel geometric characterization of conditions for linear convergence, and it clarifies the relation between the noise amplification and convergence rate as well as their dependence on the condition number and the constant algorithmic parameters. This geometric insight leads to simple alternative proofs of standard convergence results and allows us to establish analytical lower bounds on the product between the settling time and noise amplification that scale quadratically with the condition number. Our analysis also identifies a key difference between the gradient and iterate noise models: while the amplification of gradient noise can be made arbitrarily small by sufficiently decelerating the algorithm, the best achievable variance amplification for the iterate noise model increases linearly with the settling time in decelerating regime. Furthermore, we introduce two parameterized families of algorithms that strike a balance between noise amplification and settling time while preserving order-wise Pareto optimality for both noise models. Finally, by analyzing a class of accelerated gradient flow dynamics, whose suitable discretization yields the two-step momentum algorithm, we establish that stochastic performance tradeoffs also extend to continuous time.

## Index Terms

First-order algorithms, convergence rate, convex optimization, heavy-ball method, noise amplification, Nesterov’s accelerated algorithm, performance tradeoffs, settling time.

## I. INTRODUCTION

Accelerated first-order algorithms [1]–[3] are often used for solving large-scale optimization problems [4]–[6] because of their scalability, fast convergence, and low per-iteration complexity. Convergence properties of these algorithms have been carefully studied [7]–[14], but their performance in the presence of noise has received less attention [15]–[19]. Prior studies indicate that inaccuracies in the computation of gradient values can adversely impact the convergence rate of accelerated methods and that gradient descent may have advantages relative to its accelerated variants in noisy environments [20]–[24]. In contrast to gradient descent, accelerated algorithms can also exhibit undesirable transient behavior [25]–[27]; for convex quadratic problems, the non-normal dynamic modes in accelerated algorithms induce large transient responses of the error in the optimization variable [27].

Analyzing the performance of accelerated algorithms with additive white noise that arises from uncertainty in gradient evaluation dates back to [15] where Polyak established the optimal linear convergence rate for strongly convex quadratic problems. In addition, he used time-varying parameters to obtain convergence in the error variance at a sub-linear rate and with an improved constant factor compared to gradient descent. Acceleration in a sub-linear regime can also be achieved for smooth strongly convex problems with properly diminishing stepsize [28] and averaging techniques can be used to prevent the accumulation of gradient noise by accelerated algorithms [29]. For standard accelerated methods with constant parameters, control-theoretic tools were utilized in [30] and [31] to study the steady-state variance of the error in optimization variable for smooth strongly convex problems. In particular, for the parameters that optimize convergence rates for quadratic problems, tight upper and lower bounds on the noise amplification of gradient descent, heavy-ball method, and Nesterov’s accelerated algorithm were developed in [30]. These bounds are expressed in terms of the condition number  $\kappa$  and the problem dimension  $n$ , and they demonstrate opposite trends relative to the settling time: *for a fixed problem dimension  $n$ , accelerated algorithms increase noise amplification by a factor of  $\Theta(\sqrt{\kappa})$  relative to gradient descent.* Similar result also holds for heavy-ball and Nesterov’s algorithms with parameters that provide convergence rate  $\rho \leq 1 - c/\sqrt{\kappa}$  with  $c > 0$  [30]. Furthermore,

Financial support from the National Science Foundation under Awards ECCS 1708906 and ECCS 1809833 is gratefully acknowledged.

Hesameddin Mohammadi and Mihailo R. Jovanović are with the Ming Hsieh Department of Electrical and Computer Engineering, University of Southern California, Los Angeles, CA 90089, USA. Meisam Razaviyayn is with the Daniel J. Epstein Department of Industrial and Systems Engineering, University of Southern California, Los Angeles, CA 90089, USA (e-mails: hesamedm@usc.edu; mihailo@usc.edu; razaviya@usc.edu).

for all strongly convex optimization problems with a condition number  $\kappa$ , tight and attainable upper bounds for noise amplification of gradient descent and Nesterov’s accelerated method were provided in [30].

In this paper, we extend the results of [30] to the class of first-order algorithms with three constant parameters in which the iterations involve information from the two previous steps. This class includes heavy-ball and Nesterov’s accelerated algorithms as special cases and we examine its stochastic performance for strongly convex quadratic problems. Our results are complementary to [32], which evaluates stochastic performance in the objective error, and to a recent work [31] which studies the steady-state variance of the error associated with the point at which the gradient is evaluated. This reference combines theory with computational experiments to demonstrate that a parameterized family of heavy-ball-like methods with reduced stepsize provides Pareto-optimal algorithms for simultaneous optimization of convergence rate and amplification of gradient noise. In contrast to [31], we establish analytical lower bounds on the product of the settling time and the steady-state variance of the error in the optimization variable that hold for any constant stabilizing parameters and for both gradient and iterate noise models. Our lower bounds scale with the square of the condition number and reveal a fundamental limitation of this class of algorithms.

In addition to considering noise in gradient evaluation, we study the stochastic performance of algorithms when noise is directly added to the iterates (rather than the gradient). For the iterate noise model, we establish an alternative lower bound on the noise amplification which scales linearly with the settling time and is order-wise tight for settling times that are larger than that of gradient descent with the standard stepsize. In this decelerated regime, our results identify a key difference between the two noise models: while the impact of gradient uncertainties on variance amplification can be made arbitrarily small by decelerating the two-step momentum algorithm, the best achievable variance amplification for the iterate noise model increases linearly with the settling time in the decelerated regime.

Our results build upon a simple, yet powerful geometric viewpoint, which clarifies the relation between condition number, convergence rate, and algorithmic parameters for strongly convex quadratic problems. This viewpoint allows us to present alternative proofs for (i) the optimal convergence rate of the two-step momentum algorithm, which recovers Nesterov’s fundamental lower bound on the convergence rate [33] for finite dimensional problems [34]; and (ii) the optimal rates achieved by standard gradient descent, heavy-ball method, and Nesterov’s accelerated algorithm [10]. In addition, it enables a novel geometric characterization of noise amplification in terms of stability margins and it allows us to precisely quantify tradeoffs between convergence rate and robustness to noise.

We also introduce two parameterized families of algorithms that are structurally similar to the heavy-ball and Nesterov’s accelerated algorithms. These algorithms utilize continuous transformations from gradient descent to the corresponding accelerated algorithm (with the optimal convergence rate) via a homotopy path, and they can be used to provide additional insight into the tradeoff between convergence rate and noise amplification. We prove that these parameterized families are order-wise (in terms of the condition number) Pareto-optimal for simultaneous minimization of settling time and noise amplification. Another family of algorithms that facilitates similar tradeoff was proposed in [12], and it includes the fastest known algorithm for the class of smooth strongly convex problems. We also utilize negative momentum parameters to decelerate a heavy-ball-like family of algorithms relative to gradient descent with the optimal stepsize. For both noise models, our parameterized family yields order-wise optimal algorithms and it allows us to further highlight the key difference between them in the decelerated regime.

Finally, we examine the noise amplification of a class of stochastically-forced momentum-based accelerated gradient flow dynamics. Such dynamics were introduced in [35] as a continuous-time variant of Nesterov’s accelerated algorithm and a Lyapunov-based method was used to establish their stability properties and infer the convergence rate. Inspired by this work, we examine the tradeoffs between the noise amplification and convergence rate of similar gradient flow dynamics for strongly convex quadratic problems. We introduce a geometric viewpoint analogous to the discrete-time setting to characterize the optimal convergence rate and identify the corresponding algorithmic parameters. We then examine the dependence of the noise amplification on the parameters and the spectrum of the Hessian matrix and demonstrate that our findings regarding the restrictions imposed by the condition number on the product of the settling time and noise amplification extend to the continuous-time case as well.

The rest of the paper is organized as follows. In Section II, we provide preliminaries and background material and, in Section III, we summarize our key contributions. In Section IV, we introduce the tools and ideas that enable our analysis. In particular, we utilize the Jury stability criterion to provide a novel geometric characterization of stability and  $\rho$ -linear convergence and exploit this insight to derive simple alternative proofs of standard convergence results and quantify fundamental stochastic performance tradeoffs. In Section V, we introduce two parameterized families of algorithms that allow us to constructively tradeoff settling time and noise amplification. In Section VI, we extend our results to the continuous-time setting, in Section VII, we provide proofs of our main results, and in Section VIII, we conclude the paper.

## II. PRELIMINARIES AND BACKGROUND

For the unconstrained optimization problem

$$\underset{x}{\text{minimize}} \quad f(x) \quad (1)$$

where  $f: \mathbb{R}^n \rightarrow \mathbb{R}$  is a strongly convex function with a Lipschitz continuous gradient  $\nabla f$ , we consider noisy momentum-based first-order algorithms that use information from the two previous steps to update the optimization variable:

$$x^{t+2} = x^{t+1} + \beta(x^{t+1} - x^t) - \alpha \nabla f(x^{t+1} + \gamma(x^{t+1} - x^t)) + \sigma_w w^t. \quad (2)$$

Here,  $t$  is the iteration index,  $\alpha$  is the stepsize,  $\beta$  and  $\gamma$  are momentum parameters,  $\sigma_w$  is the noise magnitude, and  $w^t$  is an additive white noise with zero mean and identity covariance matrix,

$$\mathbb{E}[w^t] = 0, \quad \mathbb{E}[w^t(w^\tau)^T] = I \delta(t - \tau)$$

where  $\delta$  is the Kronecker delta and  $\mathbb{E}$  is the expected value operator. In this paper, we consider two noise models.

- 1) Iterate noise ( $\sigma_w = \sigma$ ): models uncertainty in computing the iterates of (2), where  $\sigma$  denotes the stepsize-independent noise magnitude.
- 2) Gradient noise ( $\sigma_w = \alpha\sigma$ ): models uncertainty in the gradient evaluation. In this case, the stepsize  $\alpha$  directly impacts magnitude of the additive noise.

Iterate noise models scenarios where uncertainties in optimization variables exist because of roundoff, quantization, and communication errors. This model has also been used to improve generalization and robustness in machine learning [36]. On the other hand, the second noise model accounts for gradient computation error or scenarios in which the gradient is estimated from noisy measurements [37]. Also, noise may be intentionally added to the gradient for privacy reasons [38].

*Remark 1:* An alternative noise model with  $\sigma_w = \sqrt{\alpha}\sigma$  has been used to escape local minima in stochastic gradient descent [39] and to provide non-asymptotic guarantees in non-convex learning [40], [41]. This model arises from a discretization of the continuous-time Langevin diffusion dynamics [40] and, for strongly convex quadratic problems, our framework can be used to examine acceleration/robustness tradeoffs. For algorithms that are faster than the standard gradient descent, this model has order-wise identical performance bounds as the other two models and the only difference arises in decelerated regime. We omit details for brevity.

Special cases of (2) include noisy gradient descent ( $\beta = \gamma = 0$ ), Polyak's heavy-ball method ( $\gamma = 0$ ), and Nesterov's accelerated algorithm ( $\gamma = \beta$ ). In the absence of noise (i.e., for  $\sigma = 0$ ), the parameters  $(\alpha, \beta, \gamma)$  can be selected such that the iterates converge linearly to the globally optimal solution [9]. For the family of smooth strongly convex problems, the parameters that yield the fastest known linear convergence rate were provided in [13].

### A. Linear dynamics for quadratic problems

Let  $\mathcal{Q}_m^L$  denote the class of  $m$ -strongly convex  $L$ -smooth quadratic functions

$$f(x) = \frac{1}{2} x^T Q x - q^T x \quad (3)$$

with the condition number  $\kappa := L/m$ , where  $q$  is a vector and  $Q = Q^T \succ 0$  is the Hessian matrix with eigenvalues

$$L = \lambda_1 \geq \lambda_2 \geq \dots \geq \lambda_n = m > 0.$$

For the quadratic objective function in (3), we can use a linear time-invariant (LTI) state-space model to describe the *two-step momentum algorithm* (2) with constant parameters,

$$\begin{aligned} \psi^{t+1} &= A \psi^t + B w^t \\ z^t &= C \psi^t \end{aligned} \quad (4a)$$

where  $\psi^t$  is the state,  $z^t := x^t - x^*$  is the performance output, and  $w^t$  is the white stochastic input. In particular, choosing  $\psi^t := [(x^t - x^*)^T (x^{t+1} - x^*)^T]^T$  yields

$$\begin{aligned} A &= \begin{bmatrix} 0 & I \\ -\beta I + \gamma \alpha Q & (1 + \beta)I - (1 + \gamma)\alpha Q \end{bmatrix} \\ B^T &= [ 0 \quad \sigma_w I ], \quad C = [ I \quad 0 ]. \end{aligned} \quad (4b)$$

method	fastest parameters $(\alpha, \beta, \gamma)$	$T_s$	$J_{\min}/\sigma_w^2$	$J_{\max}/\sigma_w^2$
Gradient	$(2/(L+m), 0, 0)$	$(\kappa+1)/2$	$\Theta(\kappa) + n$	$n\Theta(\kappa)$
Heavy-ball	$(4/(\sqrt{L} + \sqrt{m})^2, (1 - 2/(\sqrt{\kappa} + 1))^2, 0)$	$(\sqrt{\kappa} + 1)/2$	$\Theta(\kappa\sqrt{\kappa}) + n\Theta(\sqrt{\kappa})$	$n\Theta(\kappa\sqrt{\kappa})$
Nesterov	$(4/(3L+m), 1 - 4/(\sqrt{3\kappa+1} + 2), \beta)$	$\sqrt{3\kappa+1}/2$	$\Theta(\kappa\sqrt{\kappa}) + n$	$n\Theta(\kappa\sqrt{\kappa})$

Table I

SETTLING TIMES  $T_s := 1/(1-\rho)$  [10, PROPOSITION 1] ALONG WITH THE CORRESPONDING NOISE AMPLIFICATION BOUNDS IN (10) [30, THEOREM 4] FOR THE PARAMETERS THAT OPTIMIZE THE LINEAR CONVERGENCE RATE  $\rho$  FOR STRONGLY CONVEX QUADRATIC FUNCTION  $f \in \mathcal{Q}_m^L$  WITH THE CONDITION NUMBER  $\kappa := L/m$ , HERE,  $n$  IS THE DIMENSION OF  $x$  AND  $\sigma_w^2$  IS THE VARIANCE OF THE WHITE NOISE.

### B. Convergence rates

An algorithm is stable if in the absence of noise (i.e.,  $\sigma_w = 0$ ), the state converges linearly with some rate  $\rho < 1$ ,

$$\|\psi^t\|_2 \leq c\rho^t \|\psi^0\|_2 \text{ for all } t \geq 1 \quad (5)$$

for all  $f \in \mathcal{Q}_m^L$  and all initial conditions  $\psi^0$ , where  $c > 0$  is a constant. For LTI system (4a), the spectral radius  $\rho(A)$  determines the best achievable convergence rate. In addition,

$$T_s := \frac{1}{1-\rho} \quad (6)$$

determines the *settling time*, i.e., the number of iterations required to reach a given desired accuracy; see Appendix A. For the class  $\mathcal{Q}_m^L$  of high-dimensional functions (i.e., for  $n \gtrsim T_s$ ), Nesterov established the fundamental lower bound on the settling time (convergence rate) of any first-order algorithm [9],

$$T_s \geq \frac{\sqrt{\kappa} + 1}{2}. \quad (7)$$

This lower bound is sharp and it is achieved by the heavy-ball method with the parameters provided in Table I [10].

### C. Noise amplification

For LTI system (4a) driven by an additive white noise  $w^t$ ,  $\mathbb{E}(\psi^{t+1}) = A\mathbb{E}(\psi^t)$ . Thus,  $\mathbb{E}(\psi^t) = A^t\mathbb{E}(\psi^0)$  and, for any stabilizing parameters  $(\alpha, \beta, \gamma)$ , the iterates reach a statistical steady-state with  $\lim_{t \rightarrow \infty} \mathbb{E}(\psi^t) = 0$  and a variance that can be computed from the solution of the algebraic Lyapunov equation [30], [42]. We call the steady-state variance of the error in the optimization variable noise (or variance) amplification,

$$J := \lim_{t \rightarrow \infty} \frac{1}{t} \sum_{k=0}^t \mathbb{E}(\|x^k - x^*\|_2^2). \quad (8)$$

In addition to the algorithmic parameters  $(\alpha, \beta, \gamma)$ , the entire spectrum  $\{\lambda_i | i = 1, \dots, n\}$  of the Hessian matrix  $Q$  impacts the noise amplification  $J$  of algorithm (2) [30].

*Remark 2:* An alternative performance metric that examines the steady-state variance of  $y^t - x^*$  was considered in [31], where  $y^t := x^t + \gamma(x^t - x^{t-1})$  is the point at which the gradient is evaluated in (2). For all  $\gamma \geq 0$ , we have  $J_x \leq J_y \leq (1 + 2\gamma)^2 J_x$ , where the subscripts  $x$  and  $y$  denote the noise amplification in terms of the error in  $x^t$  and  $y^t$ . Thus, these performance metrics are within a constant factor of each other for bounded values of  $\gamma \geq 0$ .

### D. Parameters that optimize convergence rate

For special instances of the two-step momentum algorithm (2) applied to strongly convex quadratic problems, namely gradient descent (gd), heavy-ball method (hb), and Nesterov's accelerated algorithm (na), the parameters that yield the fastest convergence rates were established in [10], [15]. These parameters along with the corresponding rates and the noise amplification bounds are provided in Table I. The convergence rates are determined by the spectral radius of the corresponding  $A$ -matrices and the noise amplification bounds are computed by examining the solution to the algebraic Lyapunov equation and determining the functions  $f \in \mathcal{Q}_m^L$  for which the steady-state variance is maximized/minimized [30, Proposition 1]. Since the optimal convergence rate for the heavy-ball method meets the fundamental lower bound (7), this choice of parameters also optimizes the convergence rate of the two-step momentum algorithm (2) for  $f \in \mathcal{Q}_m^L$ .

For the optimal parameters provided in Table I, there is a  $\Theta(\sqrt{\kappa})$  improvement in settling times of the heavy-ball and Nesterov's accelerated algorithms relative to gradient descent,

$$T_s = \begin{cases} \Theta(\kappa) & \text{gd} \\ \Theta(\sqrt{\kappa}) & \text{hb, na} \end{cases} \quad (9)$$

where  $a = \Theta(b)$  means that  $a$  lies within constant factors of  $b$  as  $b \rightarrow \infty$ . This improvement makes accelerated algorithms popular for problems with large condition number  $\kappa$ .

While convergence rate is only affected by the largest and smallest eigenvalues of  $Q$ , the entire spectrum of  $Q$  influences the noise amplification  $J$ . On the other hand, the largest and smallest values of  $J$  over the function class  $\mathcal{Q}_m^L$ ,

$$J_{\max} := \max_{f \in \mathcal{Q}_m^L} J, \quad J_{\min} := \min_{f \in \mathcal{Q}_m^L} J \quad (10)$$

depend only on the noise magnitude  $\sigma_w$ , the algorithmic parameters  $(\alpha, \beta, \gamma)$ , the problem dimension  $n$ , and the extreme eigenvalues  $m$  and  $L$  of  $Q$ .

For the parameters that optimize convergence rates, tight upper and lower bounds on the noise amplification were developed in [30, Theorem 4]. These bounds are expressed in terms of the condition number  $\kappa$  and the problem dimension  $n$ , and they demonstrate opposite trends relative to the settling time. In particular, for gradient descent,

$$J_{\max} = \sigma_w^2 n \Theta(\kappa), \quad J_{\min} = \sigma_w^2 (\Theta(\kappa) + n) \quad (11a)$$

and for accelerated algorithms,

$$J_{\max} = \sigma_w^2 n \Theta(\kappa \sqrt{\kappa}), \quad J_{\min} = \begin{cases} \sigma_w^2 (\Theta(\kappa \sqrt{\kappa}) + n \Theta(\sqrt{\kappa})) & \text{hb} \\ \sigma_w^2 (\Theta(\kappa \sqrt{\kappa}) + n) & \text{na.} \end{cases} \quad (11b)$$

Thus, for fixed problem dimension  $n$  and noise magnitude  $\sigma_w$ , accelerated algorithms increase noise amplification by a factor of  $\Theta(\sqrt{\kappa})$  relative to gradient descent for the parameters that optimize convergence rates. While similar result also holds for heavy-ball and Nesterov's algorithms with arbitrary values of parameters  $\alpha$  and  $\beta$  that provide settling time  $T_s \leq c\sqrt{\kappa}$  with  $c > 0$  [30, Theorem 8], in this paper we establish fundamental tradeoffs between noise amplification and settling time for the class of the two-step momentum algorithms (2) with arbitrary stabilizing values of constant parameters  $(\alpha, \beta, \gamma)$ .

### III. SUMMARY OF MAIN RESULTS

In this section, we summarize our key contributions regarding robustness/convergence tradeoff for noisy two-step momentum algorithm (2). In addition, our geometric characterization of stability and  $\rho$ -linear convergence allows us to provide alternative proofs of standard convergence results and quantify fundamental performance tradeoffs. The proofs of results presented here can be found in Section VII.

#### A. Bounded noise amplification for stabilizing parameters

For a discrete-time LTI system with a convergence rate  $\rho$ , the distance of the eigenvalues to the unit circle is lower bounded by  $1 - \rho$ . We use this stability margin to establish an upper bound on the noise amplification  $J$  of the two-step momentum method (2) for *any* stabilizing parameters  $(\alpha, \beta, \gamma)$ .

*Theorem 1:* Let the parameters  $(\alpha, \beta, \gamma)$  be such that the two-step momentum algorithm (2) converges linearly with the rate  $\rho = 1 - 1/T_s$  for all  $f \in \mathcal{Q}_m^L$ . Then,

$$J \leq \frac{\sigma_w^2 (1 + \rho^2)}{(1 + \rho)^3} n T_s^3 \quad (12a)$$

where  $n$  is the problem size. Furthermore, for the gradient noise model ( $\sigma_w = \alpha\sigma$ ),

$$J \leq \frac{\sigma^2 (1 + \rho)(1 + \rho^2)}{L^2} n T_s^3. \quad (12b)$$

For  $\rho < 1$ , both upper bounds in (12) scale with  $n T_s^3$  and they are exact for the heavy-ball method with the parameters that optimize the convergence rate provided by Table I. However, these bounds are not tight for all stabilizing parameters; e.g., applying (12a) to gradient descent with the optimal stepsize  $\alpha = 2/(L + m)$  yields  $J \leq \sigma_w^2 n \Theta(\kappa^3)$ , which is off by a factor of  $\kappa^2$ ; cf. Table I. The bound in (12b) is obtained by combining (12a) with  $\alpha L \leq (1 + \rho)^2$ , which follows from the conditions for  $\rho$ -linear convergence in Section IV.

### B. Tradeoff between settling time and noise amplification

In this subsection, we establish lower bounds on the products  $J_{\max} \times T_s$  and  $J_{\min} \times T_s$  for any stabilizing constant parameters  $(\alpha, \beta, \gamma)$  in the two-step momentum algorithm (2), where  $J_{\max}$  and  $J_{\min}$  defined in (10) are the largest and the smallest noise amplification for the class of functions  $\mathcal{Q}_m^L$  and  $T_s$  is the settling time.

*Theorem 2:* Let the parameters  $(\alpha, \beta, \gamma)$  be such that the two-step momentum algorithm (2) converges linearly with the rate  $\rho = 1 - 1/T_s$  for all  $f \in \mathcal{Q}_m^L$ . Then,  $J_{\max}$  and  $J_{\min}$  in (10) satisfy,

$$J_{\max} \times T_s \geq \sigma_w^2 \left( (n-1) \frac{\kappa^2}{64} + \frac{\sqrt{\kappa} + 1}{2} \right) \quad (13a)$$

$$J_{\min} \times T_s \geq \sigma_w^2 \left( \frac{\kappa^2}{64} + (n-1) \frac{\sqrt{\kappa} + 1}{2} \right). \quad (13b)$$

Furthermore, for the gradient noise model ( $\sigma_w = \alpha\sigma$ ), we have

$$J_{\max} \times T_s \geq \frac{\sigma^2}{L^2} \left( (n-1) \frac{\kappa^2}{4} + \max \left\{ \frac{\kappa^2}{T_s^3}, \frac{1}{4} \right\} \right) \quad (13c)$$

$$J_{\min} \times T_s \geq \frac{\sigma^2}{L^2} \left( \frac{\kappa^2}{4} + (n-1) \max \left\{ \frac{\kappa^2}{T_s^3}, \frac{1}{4} \right\} \right). \quad (13d)$$

For both noise models, the condition number  $\kappa$  restricts the performance of the two-step momentum algorithm with constant parameters: *for a fixed problem size  $n$ , all four lower bounds in (13) scale with  $\kappa^2$* . Relative to the dominant term in  $\kappa$ , the problem dimension  $n$  appears in a multiplicative fashion for the lower bounds on  $J_{\max}$  and in an additive fashion for the lower bounds on  $J_{\min}$ . Next, by establishing upper bounds on  $J_{\max} \times T_s$  and  $J_{\min} \times T_s$  for a parameterized family of heavy-ball-like algorithms in Theorem 3, we prove that for any settling time  $T_s$  these bounds are *order-wise tight* (in  $\kappa$ ) for the gradient noise model. On the other hand, for the iterate noise model, they are tight only if  $T_s$  is smaller than the best achievable settling time of gradient descent,  $(\kappa + 1)/2$ .

*Theorem 3:* For the class of strongly convex quadratic functions  $\mathcal{Q}_m^L$  with the condition number  $\kappa = L/m$ , let the scalar  $\rho$  be such that the fundamental lower bound  $T_s = 1/(1 - \rho) \geq (\sqrt{\kappa} + 1)/2$  given by (7) holds. Then, the two-step momentum algorithm (2) with parameters

$$\alpha = \frac{(1 + \rho)(1 + \beta/\rho)}{L}, \quad \beta = \rho \frac{\kappa - (1 + \rho)/(1 - \rho)}{\kappa + (1 + \rho)/(1 - \rho)}, \quad \gamma = 0 \quad (14)$$

converges linearly with the rate  $\rho$  and, for settling times  $T_s \leq (\kappa + 1)/2$ ,  $J_{\max}$  and  $J_{\min}$  in (10) satisfy

$$J_{\max} \times T_s \leq \sigma_w^2 n \kappa (\kappa + 1)/2 \quad (15a)$$

$$J_{\min} \times T_s \leq \sigma_w^2 \kappa (\kappa + n - 1). \quad (15b)$$

Furthermore, for the gradient noise model ( $\sigma_w = \alpha\sigma$ ) and any settling time that satisfies (7), parameters (14) lead to

$$J_{\max} \times T_s \leq \sigma^2 n \kappa (\kappa + 1)/L^2 \quad (15c)$$

$$J_{\min} \times T_s \leq \sigma^2 2\kappa (\kappa + 4n - 7)/L^2. \quad (15d)$$

Theorem 3 provides upper bounds on  $J_{\max} \times T_s$  and  $J_{\min} \times T_s$  for a family of heavy-ball-like algorithms ( $\gamma = 0$ ) parameterized by the settling time  $T_s$ . For both noise models, the upper bounds in (15) scale with  $\kappa^2$  which matches the corresponding lower bounds in (13). For the gradient noise model, the upper and lower bounds are order-wise tight (in  $\kappa$ ) for any settling time. However, for the iterate noise model, the lower bounds in Theorem 2 can be improved when  $T_s \geq (\kappa + 1)/2$ . In Theorem 4, we establish alternative lower bounds on  $J_{\max}$  and  $J_{\min}$  that scale with  $T_s$  for the two-step momentum algorithm (2) with any stabilizing parameters. We also utilize parameterized family (14) of heavy-ball-like algorithms with negative momentum parameter  $\beta$  to increase  $T_s$  beyond  $(\kappa + 1)/2$  and obtain upper bounds on  $J_{\max}$  and  $J_{\min}$  that scale linearly with  $T_s$  for the iterate noise model.

*Theorem 4:* Let the parameters  $(\alpha, \beta, \gamma)$  be such that the two-step momentum algorithm (2) achieves the convergence rate  $\rho = \rho(A) = 1 - 1/T_s$ , where the matrix  $A$  is given by (4). Then,  $J_{\max}$  and  $J_{\min}$  in (10) satisfy,

$$J_{\max} \geq \sigma_w^2 \left( (n-1) \frac{T_s}{2(1+\rho)^2} + 1 \right) \quad (16a)$$

$$J_{\min} \geq \sigma_w^2 \left( \frac{T_s}{2(1+\rho)^2} + (n-1) \right). \quad (16b)$$

Furthermore, for the parameterized family of heavy-ball-like algorithms (14) with  $T_s \geq (\kappa + 1)/2$ ,

$$J_{\max} \leq \sigma_w^2 n T_s \quad (17a)$$

$$J_{\min} \leq 2\sigma_w^2 (1 + (n-2)/\kappa) T_s. \quad (17b)$$

We note that the condition  $T_s \geq (\kappa + 1)/2$  in Theorem 4 corresponds to non-positive momentum parameter  $\beta \leq 0$ . We also observe that both upper and lower bounds on  $J_{\max}$  and  $J_{\min}$  in Theorem 4 grow linearly with  $T_s$  and that for the iterate noise model with  $T_s \geq (\kappa + 1)/2$  the lower bound is sharper than the one established in Theorem 2.

*Remark 3:* Since  $\mathcal{Q}_m^L$  is a subset of the class of  $m$ -strongly convex functions with  $L$ -Lipschitz continuous gradients, the fundamental lower bounds on  $J_{\max} \times T_s$  established in Theorem 2 carry over to this broader class of problems. Thus, the restriction imposed by the condition number on the tradeoff between settling time and noise amplification goes beyond  $\mathcal{Q}_m^L$  and holds for general strongly convex problems.

*Remark 4:* The upper bounds in Theorems 3 and 4 are obtained for a particular choice of constant parameters. Thus, they also provide upper bounds on the best achievable noise amplification bounds  $J_{\max}^* := \min_{\alpha, \beta, \gamma} J_{\max}$  and  $J_{\min}^* := \min_{\alpha, \beta, \gamma} J_{\min}$  for a settling time  $T_s$ ; see Figure 1.

#### IV. CONVERGENCE AND NOISE AMPLIFICATION: GEOMETRIC CHARACTERIZATION

In this section, we examine the relation between the convergence rate and noise amplification of the two-step momentum algorithm (2) for strongly convex quadratic problems. In particular, the eigenvalue decomposition of the Hessian matrix  $Q$  allows us to bring the dynamics into  $n$  decoupled second-order systems parameterized by the eigenvalues of  $Q$  and the algorithmic parameters  $(\alpha, \beta, \gamma)$ . We utilize the Jury stability criterion to provide a novel geometric characterization of stability and  $\rho$ -linear convergence and exploit this insight to derive alternative proofs of standard convergence results and quantify fundamental performance tradeoffs.

##### A. Modal decomposition

We utilize the eigenvalue decomposition of the Hessian matrix  $Q = Q^T \succ 0$ ,  $Q = V\Lambda V^T$ , where  $\Lambda$  is the diagonal matrix of the eigenvalues and  $V$  is the orthogonal matrix of the corresponding eigenvectors. The change of variables  $\hat{x}^t := V^T(x^t - x^*)$  and  $\hat{w}^t := V^T w^t$  allows us to bring (4) into  $n$  decoupled second-order subsystems,

$$\begin{aligned} \hat{\psi}_i^{t+1} &= \hat{A}_i \hat{\psi}_i^t + \hat{B}_i \hat{w}_i^t \\ \hat{z}_i^t &= \hat{C}_i \hat{\psi}_i^t \end{aligned} \quad (18a)$$

where  $\hat{w}_i^t$  is the  $i$ th component of the vector  $\hat{w}^t \in \mathbb{R}^n$ ,  $\hat{\psi}_i^t = [\hat{x}_i^t \ \hat{x}_i^{t+1}]^T$ ,

$$\hat{A}_i = \hat{A}(\lambda_i) := \begin{bmatrix} 0 & 1 \\ -a(\lambda_i) & -b(\lambda_i) \end{bmatrix}, \quad \hat{B}_i = [0 \ \sigma_w]^T, \quad \hat{C}_i = [1 \ 0] \quad (18b)$$

and

$$a(\lambda) := \beta - \gamma\alpha\lambda, \quad b(\lambda) := (1 + \gamma)\alpha\lambda - (1 + \beta). \quad (18c)$$

##### B. Conditions for linear convergence

For the class of strongly convex quadratic functions  $\mathcal{Q}_m^L$ , the best convergence rate  $\rho$  is determined by the largest spectral radius of the matrices  $\hat{A}(\lambda)$  in (18) for  $\lambda \in [m, L]$ ,

$$\rho = \max_{\lambda \in [m, L]} \rho(\hat{A}(\lambda)). \quad (19)$$

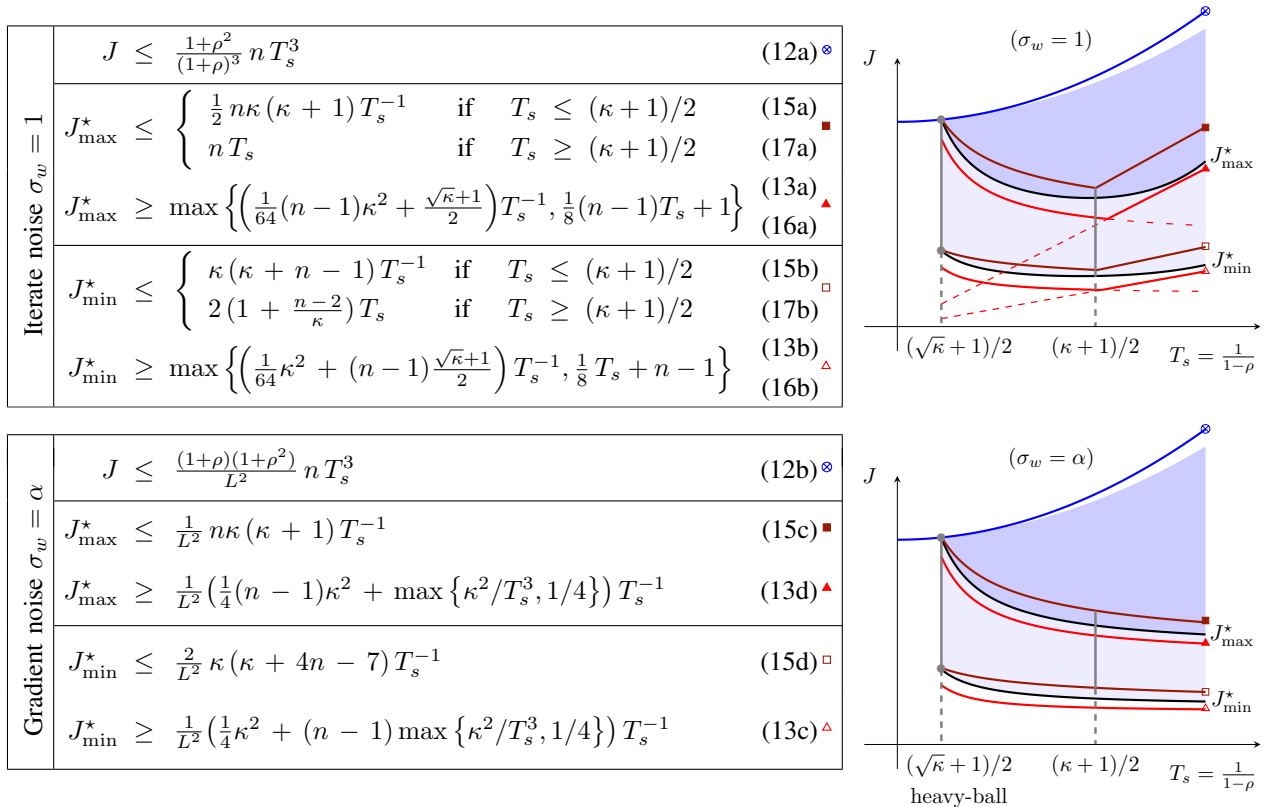


Figure 1. Summary of the results established in Theorems 1-4 for  $\sigma^2 = 1$ . The top and bottom rows correspond to the iterate and gradient noise models, respectively, and they illustrate (i)  $J_{\max}^* := \min_{\alpha, \beta, \gamma} \max_f J$  and  $J_{\min}^* := \min_{\alpha, \beta, \gamma} \min_f J$  subject to a settling time  $T_s$  for  $f \in \mathcal{Q}_m^L$  (black curves); and (ii) their corresponding upper (maroon curves) and lower (red curves) bounds in terms of the condition number  $\kappa = L/m$ , problem size  $n$ , and settling time  $T_s$ . The upper bounds on  $J$  established in Theorem 1 are marked by blue curves. The dark shaded region and its union with the light shaded region respectively correspond to all possible pairs  $(T_s, \max_f J)$  and  $(T_s, \min_f J)$  for  $f \in \mathcal{Q}_m^L$  and any stabilizing parameters  $(\alpha, \beta, \gamma)$ .

For the heavy-ball and Nesterov's accelerated methods, analytical expressions for  $\rho(\hat{A}(\lambda))$  were developed and algorithmic parameters that optimize convergence rate were obtained in [10]. Unfortunately, these expressions do not provide insight into the relation between convergence rates and noise amplification.

In this paper, we ask the dual question:

- For a fixed convergence rate  $\rho$ , what is the largest condition number  $\kappa$  that can be handled by the two-step momentum algorithm (2) with constant parameters  $(\alpha, \beta, \gamma)$ ?

We note that the matrices  $\hat{A}(\lambda)$  share the same structure as

$$M = \begin{bmatrix} 0 & 1 \\ -a & -b \end{bmatrix} \quad (20a)$$

with the real scalars  $a$  and  $b$  and that the characteristic polynomial associated with the matrix  $M$  is given by

$$F(z) := \det(zI - M) = z^2 + bz + a. \quad (20b)$$

We next utilize the Jury stability criterion [43, Chap. 4-3] to provide conditions for stability of the matrix  $M$  given by (20a).

*Lemma 1:* For the matrix  $M \in \mathbb{R}^{2 \times 2}$  given by (20a),

$$\rho(M) < 1 \iff (b, a) \in \Delta \quad (21a)$$



where the stability set

$$\Delta := \{(b, a) \mid |b| - 1 < a < 1\} \quad (21b)$$

is an open triangle in the  $(b, a)$ -plane with vertices

$$X = (-2, 1), \quad Y = (2, 1), \quad Z = (0, -1). \quad (21c)$$

*Proof:* The characteristic polynomial  $F(z)$  associated with the matrix  $M$  is given by (20b) and the Jury stability criterion [43, Chap. 4-3] provides necessary and sufficient conditions for stability,

$$|a| < 1, \quad F(\pm 1) = 1 \pm b + a > 0.$$

The condition  $a > -1$  is ensured by the positivity of  $F(\pm 1)$ . ■

For any  $\rho > 0$ , the spectral radius  $\rho(M)$  of the matrix  $M$  is smaller than  $\rho$  if and only if  $\rho(M/\rho)$  is smaller than 1. This observation in conjunction with Lemma 1 allow us to obtain necessary and sufficient conditions for stability with the linear convergence rate  $\rho$  of the two-step momentum algorithm (2).

*Lemma 2:* For any positive scalar  $\rho < 1$  and the matrix  $M \in \mathbb{R}^{2 \times 2}$  given by (20a), we have

$$\rho(M) \leq \rho \iff (b, a) \in \Delta_\rho \quad (22a)$$

where the  $\rho$ -linear convergence set

$$\Delta_\rho := \{(b, a) \mid \rho(|b| - \rho) \leq a \leq \rho^2\} \quad (22b)$$

is a closed triangle in the  $(b, a)$ -plane with vertices

$$X_\rho = (-2\rho, \rho^2), \quad Y_\rho = (2\rho, \rho^2), \quad Z_\rho = (0, -\rho^2). \quad (22c)$$

*Proof:* See Appendix C. ■

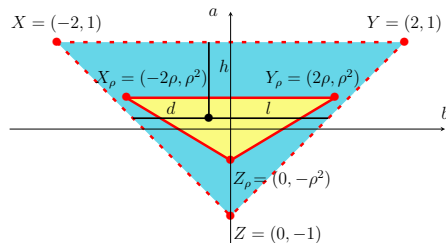


Figure 2. The stability set  $\Delta$  (the open, cyan triangle) in (21b) and the  $\rho$ -linear convergence set  $\Delta_\rho$  (the closed, yellow triangle) in (22b) along with the corresponding vertices. For the point  $(b, a)$  (black dot) associated with the matrix  $M$  in (20a), the corresponding distances  $(d, h, l)$  in (29) are marked by black lines.

Figure 2 illustrates the stability and the  $\rho$ -linear convergence sets  $\Delta$  and  $\Delta_\rho$ . We note that for any  $\rho \in (0, 1)$ , we have  $\Delta_\rho \subset \Delta$ . This can be verified by observing that the vertices  $(X_\rho, Y_\rho, Z_\rho)$  of  $\Delta_\rho$  all lie in  $\Delta$ .

For the two-step momentum algorithm (2), the functions  $a(\lambda)$  and  $b(\lambda)$  given by (18c) satisfy the affine relation,

$$(1 + \gamma)a(\lambda) + \gamma b(\lambda) = \beta - \gamma. \quad (23)$$

This fact in conjunction with Lemmas 1 and 2 allow us to derive conditions for stability and the convergence rate.

*Lemma 3:* The two-step momentum algorithm (2) with constant parameters  $(\alpha, \beta, \gamma)$  is stable for all functions  $f \in \mathcal{Q}_m^L$  if and only if the following equivalent conditions hold:

- 1)  $(b(\lambda), a(\lambda)) \in \Delta$  for all  $\lambda \in [m, L]$ ;
- 2)  $(b(\lambda), a(\lambda)) \in \Delta$  for  $\lambda \in \{m, L\}$ .

Furthermore, the linear convergence rate  $\rho < 1$  is achieved for all functions  $f \in \mathcal{Q}_m^L$  if and only if the following equivalent conditions hold:

- 1)  $(b(\lambda), a(\lambda)) \in \Delta_\rho$  for all  $\lambda \in [m, L]$ ;
- 2)  $(b(\lambda), a(\lambda)) \in \Delta_\rho$  for  $\lambda \in \{m, L\}$ .

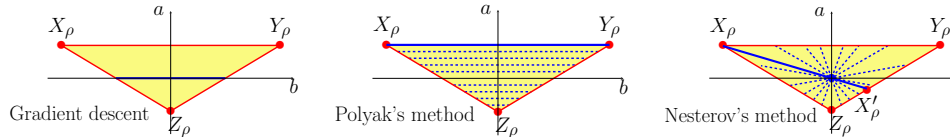


Figure 3. For a fixed  $\rho$ -linear convergence triangle  $\Delta_\rho$  (yellow), dashed blue lines mark the line segments  $(b(\lambda), a(\lambda))$  with  $\lambda \in [m, L]$  for gradient descent, Polyak's heavy-ball, and Nesterov's accelerated methods as particular instances of the two-step momentum algorithm (2) with constant parameters. The solid blue line segments correspond to the parameters for which the algorithm achieves rate  $\rho$  for the largest possible condition number given by (28).

Here,  $(b(\lambda), a(\lambda))$  is given by (18c), and the stability and  $\rho$ -linear convergence triangles  $\Delta$  and  $\Delta_\rho$  are given by (21b) and (22b), respectively.

*Proof:* The conditions in 1) follow from combining (19) with Lemma 1 (for stability) and with Lemma 2 (for  $\rho$ -linear convergence). The conditions in 2) follow from the facts that  $\Delta$  and  $\Delta_\rho$  are convex sets and that  $(b(\lambda), a(\lambda))$  is a line segment in the  $(b, a)$ -plane with end points corresponding to  $\lambda = m$  and  $\lambda = L$ . ■

Lemma 3 exploits the affine relation (23) between  $a(\lambda)$  and  $b(\lambda)$  and the convexity of the sets  $\Delta$  and  $\Delta_\rho$  to establish necessary and sufficient conditions for stability and  $\rho$ -linear convergence: *the inclusion of the end points of the line segment  $(b(\lambda), a(\lambda))$  associated with the extreme eigenvalues  $m$  and  $L$  of the matrix  $Q$  in the corresponding triangle.* A similar approach was taken in [31, Appendix A.1], where the affine nature of the conditions resulting from the Jury stability criterion with respect to  $\lambda$  was used to conclude that  $\rho(\hat{A}(\lambda))$  is a quasi-convex function of  $\lambda$  and show that the extreme points  $m$  and  $L$  determine  $\rho(A)$ . In contrast, we exploit the triangular shapes of the stability and  $\rho$ -linear convergence sets  $\Delta$  and  $\Delta_\rho$  and utilize this geometric insight to identify the parameters that optimize the convergence rate and to establish tradeoffs between noise amplification and convergence rate.

The following corollary is immediate.

*Corollary 1:* Let the two-step momentum algorithm (2) with constant parameters  $(\alpha, \beta, \gamma)$  minimize a function  $f \in \mathcal{Q}_m^L$  with a linear rate  $\rho < 1$ . Then, the convergence rate  $\rho$  is achieved for all functions  $f \in \mathcal{Q}_m^L$ .

*Proof:* Lemma 3 implies that only the extreme eigenvalues  $m$  and  $L$  of  $Q$  determine  $\rho$ . Since all functions  $f \in \mathcal{Q}_m^L$  share the same extreme eigenvalues, this completes the proof. ■

For the two-step momentum algorithm (2) with constant parameters, Lemma 3 leads to a simple alternative proof for the fundamental lower bound (7) on the settling time established by Nesterov. Our proof utilizes the fact that for any point  $(b(\lambda), a(\lambda)) \in \Delta_\rho$ , the horizontal signed distance to the edge  $XZ$  of the stability triangle  $\Delta$  satisfies

$$d(\lambda) := a(\lambda) + b(\lambda) + 1 = \alpha\lambda. \quad (24)$$

where  $a$  and  $b$  are given by (18c); see Figure 2 for an illustration.

*Proposition 1:* Let the two-step momentum algorithm (2) with constant parameters  $(\alpha, \beta, \gamma)$  achieve the linear convergence rate  $\rho < 1$  for all functions  $f \in \mathcal{Q}_m^L$ . Then, lower bound (7) on the settling time holds and it is achieved by the heavy-ball method with the parameters provided in Table I.

*Proof:* Let  $d(m) = \alpha m$  and  $d(L) = \alpha L$  denote the values of the function  $d(\lambda)$  associated with the points  $(b(m), a(m))$  and  $(b(L), a(L))$ , where  $(b, a)$  and  $d$  are given by (18c) and (24), respectively. Lemma 3 implies that  $(b(L), a(L))$  and  $(b(m), a(m))$  lie in the  $\rho$ -linear convergence triangle  $\Delta_\rho$ . Thus,

$$d_{\max}/d_{\min} \geq d(L)/d(m) = \kappa \quad (25)$$

where  $d_{\max}$  and  $d_{\min}$  are the largest and smallest values of  $d$  among all points  $(b, a) \in \Delta_\rho$ . From the shape of  $\Delta_\rho$ , we conclude that  $d_{\max}$  and  $d_{\min}$  correspond to the vertices  $Y_\rho$  and  $X_\rho$  of  $\Delta_\rho$  given by (22c); see Figure 2. Thus,

$$d_{\max} = d_{Y_\rho} = 1 + \rho^2 + 2\rho = (1 + \rho)^2 \quad (26a)$$

$$d_{\min} = d_{X_\rho} = 1 + \rho^2 - 2\rho = (1 - \rho)^2. \quad (26b)$$

Combining (25) with (26) yields

$$\kappa = \frac{d(L)}{d(m)} \leq \frac{d_{\max}}{d_{\min}} = \frac{(1 + \rho)^2}{(1 - \rho)^2}. \quad (27)$$

Rearranging terms in (27) gives lower bound (7). ■

To provide additional insight, we next examine the implications of Lemma 3 for gradient descent, Polyak's heavy-ball, and Nesterov's accelerated algorithms. In all three cases, our dual approach recovers the optimal convergence rates provided in Table I. From the affine relation (23), it follows that  $(b(\lambda), a(\lambda))$  with  $\lambda \in [m, L]$  for,

- gradient descent ( $\beta = \gamma = 0$ ), is a horizontal line segment parameterized by  $a(\lambda) = 0$ ;
- heavy-ball method ( $\gamma = 0$ ), is a horizontal line segment parameterized by  $a(\lambda) = \beta$ ; and
- Nesterov's accelerated method ( $\beta = \gamma$ ), is a line segment parameterized by  $a(\lambda) = -\beta b(\lambda)/(1 + \beta)$ .

These observations are illustrated in Figure 3 and, as we show in the proof of Lemma 3, to obtain the largest possible condition number for which the convergence rate  $\rho$  is feasible for each algorithm, one needs to find the largest ratio  $d(L)/d(m) = \kappa$  among all possible orientations for the line segment  $(b(\lambda), a(\lambda))$  with  $\lambda \in [m, L]$  to lie within  $\Delta_\rho$ . This leads to the following conditions:

- For gradient descent, the largest ratio  $d(L)/d(m)$  corresponds to the intersections of the horizontal axis and the edges  $Y_\rho Z_\rho$  and  $X_\rho Z_\rho$  of the triangle  $\Delta_\rho$ , which are given by  $(\rho, 0)$  and  $(-\rho, 0)$ , respectively. Thus, we have

$$\kappa = d(L)/d(m) \leq (1 + \rho)/(1 - \rho). \quad (28a)$$

Rearranging terms in (28a) yields a lower bound on the settling time for gradient descent  $1/(1 - \rho) \geq (\kappa + 1)/2$ . This lower bound is tight as it can be achieved by choosing the parameters in Table I, which place  $(b(\lambda), a(\lambda))$  to  $(\rho, 0)$  and  $(-\rho, 0)$  for  $\lambda = L$  and  $\lambda = m$ , respectively.

- For the heavy-ball method, the optimal rate is recovered by designing the parameters  $(\alpha, \beta)$  such that the vertices  $X_\rho$  and  $Y_\rho$  belong to the horizontal line segment  $(b(\lambda), a(\lambda))$ ,

$$\kappa = d(L)/d(m) \leq (1 + \rho)^2/(1 - \rho)^2. \quad (28b)$$

By choosing  $d(L) = d_{Y_\rho}$  and  $d(m) = d_{X_\rho}$ , we recover the optimal parameters provided in Table I and achieve the fundamental lower bound (7) on the convergence rate.

- For Nesterov's accelerated method, the largest ratio  $d(L)/d(m)$  corresponds to the line segment  $X_\rho X'_\rho$  that passes through the origin, where  $X'_\rho = (2\rho/3, -\rho^2/3)$  lies on the edge  $Y_\rho Z_\rho$ ; see Appendix C. This yields

$$\kappa = d(L)/d(m) \leq (1 + \rho)(3 - \rho)/(3(1 - \rho)^2). \quad (28c)$$

Rearranging terms in this inequality provides a lower bound on the settling time  $1/(1 - \rho) \geq \sqrt{3\kappa + 1}/2$ . This lower bound is tight and it can be achieved with the parameters provided in Table I, which place  $(b(L), a(L))$  to  $X'_\rho$  and  $(b(m), a(m))$  to  $X_\rho$ .

Figure 3 illustrates the optimal orientations discussed above.

### C. Noise amplification

To quantify the noise amplification of the two-step momentum algorithm (2), we utilize an alternative characterization of the stability and  $\rho$ -linear convergence triangles  $\Delta$  and  $\Delta_\rho$ . As illustrated in Figure 2, let  $d$  and  $l$  denote the horizontal signed distances of the point  $(a, b)$  to the edges  $XZ$  and  $YZ$  of the stability triangle  $\Delta$ ,

$$\begin{aligned} d(\lambda) &:= a(\lambda) + b(\lambda) + 1 \\ l(\lambda) &:= a(\lambda) - b(\lambda) + 1. \end{aligned} \quad (29a)$$

and let  $h$  denote its vertical signed distance to the edge  $XY$ ,

$$h(\lambda) := 1 - a(\lambda). \quad (29b)$$

Then, the following equivalence conditions,

$$(b, a) \in \Delta \iff h, d, l > 0 \quad (30a)$$

$$(b, a) \in \Delta_\rho \iff \begin{cases} h \geq (1 - \rho)(1 + \rho) \\ d \geq (1 - \rho)(1 + \rho + b) \\ l \geq (1 - \rho)(1 + \rho - b) \end{cases} \quad (30b)$$

follow from the definition of the sets  $\Delta$  in (21b),  $\Delta_\rho$  in (22b), and  $(h, d, l)$  in (29).

In Theorem 5, we quantify the steady-state variance of the error in the optimization variable in terms of the spectrum of the Hessian matrix and the algorithmic parameters for noisy two-step momentum algorithm (2). Special

cases of this result for gradient decent, heavy-ball, and Nesterov's accelerated algorithms were established in [30]. The proof of Theorem 5 follows from similar arguments and we omit it for brevity.

*Theorem 5:* For a strongly convex quadratic objective function  $f \in \mathcal{Q}_m^L$  with the Hessian matrix  $Q$ , the steady-state variance of  $x^t - x^*$  for the two-step momentum algorithm (2) with any stabilizing parameters  $(\alpha, \beta, \gamma)$  is determined by

$$J = \sum_{i=1}^n \frac{\sigma_w^2(d(\lambda_i) + l(\lambda_i))}{2d(\lambda_i)h(\lambda_i)l(\lambda_i)} =: \sum_{i=1}^n \hat{J}(\lambda_i)$$

Here,  $\hat{J}(\lambda_i)$  denotes the modal contribution of the  $i$ th eigenvalue  $\lambda_i$  of  $Q$  to the steady-state variance,  $(d, h, l)$  are defined in (29), and  $(a, b)$  are given by (18c).

In Appendix F, we describe how the algebraic Lyapunov equation for the steady-state covariance matrix of the error in the optimization variable can be used to compute the noise amplification  $J$ . Theorem 5 demonstrates that  $J$  depends on the entire spectrum of the Hessian matrix  $Q$  and not only on its extreme eigenvalues  $m$  and  $L$ , which determine the convergence rate. Since for any  $f \in \mathcal{Q}_m^L$  the extreme eigenvalues of  $Q$  are fixed at  $m$  and  $L$ , we have

$$\begin{aligned} J_{\max} &:= \max_{f \in \mathcal{Q}_m^L} J = \hat{J}(m) + \hat{J}(L) + (n-2)\hat{J}_{\max} \\ J_{\min} &:= \min_{f \in \mathcal{Q}_m^L} J = \hat{J}(m) + \hat{J}(L) + (n-2)\hat{J}_{\min} \end{aligned} \quad (31a)$$

where

$$\hat{J}_{\max} := \max_{\lambda \in [m, L]} \hat{J}(\lambda), \quad \hat{J}_{\min} := \min_{\lambda \in [m, L]} \hat{J}(\lambda). \quad (31b)$$

We use these expressions to determine explicit upper and lower bounds on  $J_{\max}$  and  $J_{\min}$  in terms of the condition number and the settling time.

## V. DESIGNING ORDER-WISE PARETO-OPTIMAL ALGORITHMS WITH ADJUSTABLE PARAMETERS

We now utilize the geometric insight developed in Section IV to design algorithmic parameters that tradeoff settling time and noise amplification. In particular, we introduce two parameterized families of heavy-ball-like ( $\gamma = 0$ ) and Nesterov-like ( $\gamma = \beta$ ) algorithms that provide *continuous transformations* from gradient descent to the corresponding accelerated algorithm (with the optimal convergence rate) via a homotopy path parameterized by the settling time  $T_s$ . For both the iterate and gradient noise models, we establish an order-wise tight scaling  $\Theta(\kappa^2)$  for  $J_{\max} \times T_s$  and  $J_{\min} \times T_s$  in accelerated regime (i.e., when  $T_s$  is smaller than the settling time of gradient descent with the optimal stepsize,  $(\kappa + 1)/2$ ). This is a direct extension of [30, Theorem 4] which studied gradient descent and its accelerated variants for the parameters that optimize the corresponding convergence rates.

We also examine performance tradeoffs for the parameterized family of heavy-ball-like algorithms with negative momentum parameter  $\beta < 0$ . This decelerated regime corresponds to settling times larger than  $(\kappa + 1)/2$  and it captures a key difference between the two noise models: *for  $T_s \geq (\kappa + 1)/2$ ,  $J_{\max}$  and  $J_{\min}$  grow linearly with the settling time  $T_s$  for the iterate noise model and they remain inversely proportional to  $T_s$  for the gradient noise model.* Comparison with the lower bounds in Theorems 2 and 4 shows that the parameterized family of heavy-ball-like methods yields order-wise optimal (in  $\kappa$  and  $T_s$ )  $J_{\max}$  and  $J_{\min}$  for both noise models. The results presented here prove all upper bounds in Theorems 3 and 4.

### A. Parameterized family of heavy-ball-like methods

For the two-step momentum algorithm (2) with  $\gamma = 0$ , the line segment  $(b(\lambda), a(\lambda))$  parameterized by  $\lambda \in [m, L]$  is parallel to the  $b$ -axis in the  $(b, a)$ -plane and it satisfies  $a(\lambda) = \beta$ . As described in Section IV, gradient descent and heavy-ball methods with the optimal parameters provided in Table I are obtained for  $\beta = 0$  and  $\beta = \rho^2$ , respectively, and the corresponding end points  $(b(m), a(m))$  and  $(b(L), a(L))$  lie at the edges  $X_\rho Z_\rho$  and  $Y_\rho Z_\rho$  of the  $\rho$ -linear convergence triangle  $\Delta_\rho$ . Inspired by this observation, we propose a family of parameters for which  $\beta = c\rho^2$ , for some scalar  $c \in [-1, 1]$ , and determine the stepsize  $\alpha$  such that the above end points lie at  $X_\rho Z_\rho$  and  $Y_\rho Z_\rho$ ,

$$\alpha = (1 + \rho)(1 + c\rho)/L, \quad \beta = c\rho^2, \quad \gamma = 0. \quad (32)$$

This yields a continuous transformation between the standard heavy-ball method ( $c = 1$ ) and gradient descent ( $c = 0$ ) for a fixed condition number  $\kappa$ . In addition, the momentum parameter  $\beta$  in (32) becomes negative for  $c < 0$ ; see

Figure 3 for an illustration. In Lemma 4, we provide expressions for the scalar  $c$  as well as for  $\hat{J}_{\max}$  and  $\hat{J}_{\min}$  defined in (31b) in terms of the condition number  $\kappa$  and the convergence rate  $\rho$ .

*Lemma 4:* For the class of functions  $\mathcal{Q}_m^L$  with the condition number  $\kappa = L/m$ , let the scalar  $\rho$  be such that

$$T_s = 1/(1 - \rho) \geq (\sqrt{\kappa} + 1)/2.$$

Then, the two-step momentum algorithm (2) with parameters (32) achieves the convergence rate  $\rho$ , and the largest and smallest values  $\hat{J}_{\max}$  and  $\hat{J}_{\min}$  of  $\hat{J}(\lambda)$  for  $\lambda \in [m, L]$  satisfy

$$\begin{aligned} \hat{J}_{\max} &= \hat{J}(m) = \hat{J}(L) = \frac{\sigma_w^2(\kappa + 1)}{2(1 - c\rho^2)(1 + \rho)(1 + c\rho)} \\ \hat{J}_{\min} &= \hat{J}(\hat{\lambda}) = \frac{\sigma_w^2}{(1 + c\rho^2)(1 - c\rho^2)} \end{aligned}$$

where  $\hat{\lambda} := (m + L)/2$  and the scalar  $c$  is given by

$$c := \frac{\kappa - (1 + \rho)/(1 - \rho)}{\rho(\kappa + (1 + \rho)/(1 - \rho))} \in [-1, 1]. \quad (33)$$

*Proof:* See Appendix D. ■

The parameters in (32) with  $c$  given by (33) are equivalent to the parameters presented in Theorem 3. Lemma 4 in conjunction with (31) allow us to derive analytical expressions for  $J_{\max}$  and  $J_{\min}$ .

*Corollary 2:* The parameterized family of heavy-ball-like methods (32) satisfies

$$\begin{aligned} J_{\max} &= n\hat{J}(m) = n\hat{J}(L) \\ J_{\min} &= 2\hat{J}(m) + (n - 2)\hat{J}(\hat{\lambda}) \end{aligned}$$

where  $\hat{J}(m)$  and  $\hat{J}(\hat{\lambda})$  are given in Lemma 4, and  $J_{\max}$  and  $J_{\min}$  defined in (10) are the largest and smallest values of  $J$  when the algorithm is applied to  $f \in \mathcal{Q}_m^L$  with the condition number  $\kappa = L/m$ .

The next proposition uses the analytical expressions in Corollary 2 to establish order-wise tight upper and lower bounds on  $J_{\max}$  and  $J_{\min}$  for the parameterized family of heavy-ball-like algorithms (32). Our upper and lower bounds are within constant factors of each other and they are expressed in terms of the problem size  $n$ , condition number  $\kappa$ , and settling time  $T_s$ .

*Proposition 2:* For the parameterized family of heavy-ball-like methods (32),  $J_{\max}$  and  $J_{\min}$  in (10) satisfy,

$$J_{\max} \times T_s = \sigma_w^2 p_{1c}(\rho) n \kappa (\kappa + 1) \quad (34a)$$

$$J_{\min} \times T_s = \sigma_w^2 \kappa (2 p_{1c}(\rho) (\kappa + 1) + (n - 2) p_{2c}(\rho)). \quad (34b)$$

Furthermore, for the gradient noise model ( $\sigma_w = \alpha\sigma$ ),

$$J_{\max} \times T_s = \sigma^2 p_{3c}(\rho) n \kappa (\kappa + 1) \quad (35a)$$

$$J_{\min} \times T_s = \sigma^2 \kappa (2 p_{3c}(\rho) (\kappa + 1) + (n - 2) p_{4c}(\rho)) \quad (35b)$$

where

$$\begin{aligned} p_{1c}(\rho) &:= q_c(\rho)/(2(1 + \rho)^2(1 + c\rho^2)), & p_{2c}(\rho) &:= q_c(\rho)/((1 + \rho)(1 + c\rho^2)(1 + c\rho)) \\ p_{3c}(\rho) &:= q_c(\rho)/(2L^2), & p_{4c}(\rho) &:= q_c(\rho)q_{-c}(\rho)(1 + \rho)/L^2 \end{aligned} \quad (36)$$

and  $q_c(\rho) := (1 - c\rho)/(1 - c\rho^2)$ . In addition, for  $c \in [0, 1]$ ,  $p_{1c}(\rho) \in [1/64, 1/2]$  and  $p_{2c}(\rho) \in [1/16, 1]$ ; and for  $c \in [-1, 1]$ ,  $p_{3c}(\rho) \in [1/(4L^2), 1/L^2]$  and  $p_{4c}(\rho) \in [1/(4L^2), 4/L^2]$ .

*Proof:* See Appendix D. ■

*Proposition 3:* For the parameterized family of heavy-ball-like methods (32) with  $c \in [-1, 0]$ ,  $J_{\max}$  and  $J_{\min}$  in (10) satisfy,

$$J_{\max} = \sigma_w^2 p_{5c}(\rho) n (1 + 1/\kappa) T_s \quad (37a)$$

$$J_{\min} = \sigma_w^2 (2 p_{5c}(\rho) (1 + 1/\kappa) + p_{6c}(\rho)(n - 2)/\kappa) T_s \quad (37b)$$

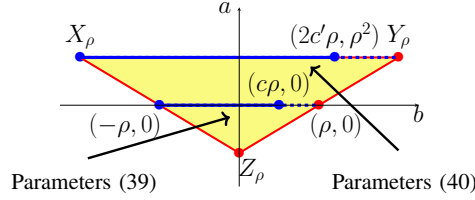


Figure 4. The triangle  $\Delta_\rho$  (yellow) and the line segments  $(b(\lambda), a(\lambda))$  with  $\lambda \in [m, L]$  (blue) for gradient descent with reduced stepsize (39) and heavy-ball-like method (40), which place the end point  $(b(m), a(m))$  at  $X_\rho$  and the end point  $(b(L), a(L))$  at  $(2c'\rho, \rho^2)$  on the edge  $X_\rho Y_\rho$ , where  $c' := \kappa(1 - \rho)^2/\rho - (1 + \rho^2)/\rho$  ranges over the interval  $[-1, 1]$ .

where  $p_{5c}(\rho) := 1/(2(1 + |c|\rho)(1 + |c|\rho^2)) \in [1/8, 1/2]$  and  $p_{6c}(\rho) := 2(1 + \rho)p_{5c}(\rho)q_{-c}(\rho) \in [1/8, 2]$ .

*Proof:* See Appendix D. ■

The upper bounds in Theorems 3 and 4 follow from Propositions 2 and 3, respectively. Since these upper bounds have the same scaling as the corresponding lower bounds in Theorems 2 and 4 that hold for all stabilizing parameters  $(\alpha, \beta, \gamma)$ , this demonstrates tightness of lower bounds for all settling times and for both noise models.

### B. Parameterized family of Nesterov-like methods

For the two-step momentum algorithm (2) with  $\gamma = \beta$ , the line segment  $(b(\lambda), a(\lambda))$  parameterized by  $\lambda \in [m, L]$  passes through the origin. As described in Section IV, gradient descent and Nesterov's method with the optimal parameters provided in Table I are obtained for  $a = 0$  and  $a = -(\rho/2)b$ , respectively, and the corresponding end points  $(b(m), a(m))$  and  $(b(L), a(L))$  lie on the edges  $X_\rho Z_\rho$  and  $Y_\rho Z_\rho$  of the  $\rho$ -linear convergence triangle  $\Delta_\rho$ . To provide a continuous transformation between these two standard algorithms, we introduce a parameter  $c \in [0, 1/2]$ , and let the line segment satisfy  $a(\lambda) = -c\rho b(\lambda)$  and take its end points at the edges  $X_\rho Z_\rho$  and  $Y_\rho Z_\rho$ ; see Figure 3 for an illustration. This can be accomplished with the following choice of parameters,

$$\alpha = (1 + \rho)(1 + c - c\rho)/(L(1 + c)), \quad \gamma = \beta = c\rho^2/((\alpha L - 1)(1 + c)). \quad (38)$$

For the parameterized family of Nesterov-like algorithms (38), Proposition 4 establishes the settling time and characterizes the dependence of  $J_{\min} \times T_s$  and  $J_{\max} \times T_s$  on the condition number  $\kappa$  and the problem size  $n$ .

*Proposition 4:* For the class of functions  $\mathcal{Q}_m^L$  with the condition number  $\kappa = L/m$ , let the scalar  $\rho$  be such that

$$T_s = 1/(1 - \rho) \in [(\sqrt{3\kappa + 1})/2, (\kappa + 1)/2].$$

The two-step momentum algorithm (2) with parameters (38) achieves the convergence rate  $\rho$  and satisfies

$$\begin{aligned} \sigma_w^2 ((n - 1)\kappa(\kappa + 1)/32 + \sqrt{3\kappa + 1}/2) &\leq J_{\max} \times T_s \leq 6\sigma_w^2 n \kappa(3\kappa + 1) \\ \sigma_w^2 (\kappa(\kappa + 1)/32 + (n - 1)\sqrt{3\kappa + 1}/2) &\leq J_{\min} \times T_s \leq \sigma_w^2 (6\kappa(3\kappa + 1) + (n - 1)(\kappa + 1)/2) \end{aligned}$$

where  $J_{\max}$  and  $J_{\min}$  are the largest and smallest values that  $J$  can take when the algorithm is applied to  $f \in \mathcal{Q}_m^L$  with the condition number  $\kappa = L/m$ , and the scalar  $c \in [0, 1/2]$  is the solution to the quadratic equation

$$\kappa(1 - \rho)(1 - c\rho - c^2(1 + \rho)) = (1 + \rho)(1 - c\rho - c^2(1 - \rho)).$$

*Proof:* See Appendix D. ■

Since the stepsize in (38) satisfies  $\alpha \in [1/L, 3/L]$ , comparing the upper bounds in Proposition 4 with the lower bounds in Theorem 2 shows that, for settling times  $T_s \leq (\kappa + 1)/2$ , the parameters in (38) achieve order-wise optimal  $J_{\max}$  and  $J_{\min}$  for both the iterate ( $\sigma_w = \sigma$ ) and gradient ( $\sigma_w = \alpha\sigma$ ) noise models.

### C. Impact of reducing the stepsize

When the only source of uncertainty is a noisy gradient, i.e.,  $\sigma_w = \alpha\sigma$ , one can attempt to reduce the noise amplification  $J$  by decreasing the stepsize  $\alpha$  at the expense of increasing the settling time  $T_s = 1/(1 - \rho)$  [14], [18], [31], [32]. In particular, for gradient descent,  $\alpha$  can be reduced from its optimal value  $2/(L + m)$  by keeping  $(b(m), a(m))$  at  $(-\rho, 0)$  and moving the point  $(b(L), a(L))$  from  $(\rho, 0)$  towards  $(-\rho, 0)$  along the horizontal axis; see Figure 4. This can be accomplished with

$$\alpha = (1 + c\rho)/L, \quad \gamma = \beta = 0 \quad (39)$$

for some  $c \in [-1, 1]$  parameterizing  $(b(L), a(L)) = (c\rho, 0)$ . In this case, the settling time satisfies  $T_s = (\kappa + c)/(c + 1) \in [(\kappa + 1/2), \infty)$  and similar arguments to those presented in the proof of Lemma 4 can be used to obtain

$$\begin{aligned} \hat{J}_{\max} &= \hat{J}(m) = \sigma^2 \kappa^2 (1 - \rho) / L^2 \\ \hat{J}_{\min} &= \begin{cases} \hat{J}(L) = \sigma^2 \alpha^2 / (1 - c^2 \rho^2) & c \leq 0 \\ \hat{J}(1/\alpha) = \sigma^2 \alpha^2 & c \geq 0. \end{cases} \end{aligned}$$

For a fixed  $n$ , the stepsize in (39) yields a  $\Theta(\kappa^2)$  scaling for both  $J_{\max} \times T_s$  and  $J_{\min} \times T_s$  for all  $c \in [-1, 1]$ . Thus, gradient descent with reduced stepsize order-wise matches the lower bounds in Theorem 2. An IQC-based approach [30, Lemma 1] was utilized in [31, Theorem 13] to show that stepsize (39) also yields the above discussed convergence rate and worst-case noise amplification for one-point  $m$ -strongly convex  $L$ -smooth functions.

*Remark 5:* Any desired settling time  $T_s = 1/(1 - \rho) \in [(\sqrt{\kappa} + 1)/2, \infty)$  can be achieved by the heavy-ball-like method with reduced stepsize,

$$\alpha = (1 - \rho)^2 / m, \quad \beta = \rho^2, \quad \gamma = 0. \quad (40)$$

This choice yields  $J_{\max} = \sigma^2 n \kappa^2 (1 - \rho^4) / (L^2 (1 + \rho)^4)$  [31, Theorem 9]; see Figure 4. In addition, by considering the error in  $y^t = x^t + \gamma(x^t - x^{t-1})$  as the performance metric, it was stated and numerically verified in [31] that the choice of parameters (40) yields Pareto-optimal algorithms for simultaneously optimizing  $J_{\max}$  and  $\rho$ . We note that the settling time  $T_s = \Theta(\kappa)$  of gradient descent with standard stepsizes ( $\alpha = 1/L$  or  $2/(m + L)$ ) can be achieved via (40) by reducing  $\alpha$  to  $O(1/(\kappa L))$ . In contrast, the parameterized family of heavy-ball-like methods (32) is order-wise Pareto-optimal (cf. Theorems 2-4) while maintaining  $\alpha \in [1/L, 4/L]$ .

## VI. CONTINUOUS-TIME GRADIENT FLOW DYNAMICS

Noisy gradient descent can be viewed as the forward Euler discretization of gradient flow dynamics (gfd),

$$\dot{x} + \alpha \nabla f(x) = \sigma w \quad (41a)$$

where  $\dot{x}$  denotes the derivative of  $x$  with respect to time  $\tau$  and  $w$  is a white noise with zero mean and identity covariance matrix,  $\mathbb{E}[w(\tau)] = 0$ ,  $\mathbb{E}[w(\tau_1)w^T(\tau_2)] = I\delta(\tau_1 - \tau_2)$ . Similarly, noisy two-step momentum algorithm (2) can be obtained by discretizing the accelerated gradient flow dynamics (agd),

$$\ddot{x} + \theta \dot{x} + \alpha \nabla f(x + \gamma \dot{x}) = \sigma w \quad (41b)$$

with  $\theta := 1 - \beta$  by approximating  $x$ ,  $\dot{x}$ , and  $\ddot{x}$  using

$$x = x^{t+1}, \quad \dot{x} \approx x^{t+1} - x^t, \quad \ddot{x} \approx x^{t+2} - 2x^{t+1} + x^t.$$

System (41b) with  $\beta = \gamma$  was introduced in [35] as a continuous-time analogue of Nesterov's accelerated algorithm and a Lyapunov-based method was employed to characterize its stability properties for smooth strongly convex problems.

For a time dilation  $s = c\tau$ , the solution to (41b) satisfies

$$x'' + \bar{\theta}x' + \bar{\alpha}\nabla f(x + \bar{\gamma}x') = \bar{\sigma}w$$

where  $\dot{x} = dx/d\tau$ ,  $x' = dx/ds$ , and

$$\bar{\theta} = \theta/c, \quad \bar{\gamma} = c\gamma, \quad \bar{\alpha} = \alpha/c^2, \quad \bar{\sigma} = \sigma/(c\sqrt{c}).$$

This follows by combining  $\dot{x} = cx'$  and  $\ddot{x} = c^2x''$  with the fact that the time dilation yields a  $\sqrt{c}$  increase in the noise magnitude  $\sigma$ . Similar change of variables can be applied to gradient flow dynamics (41a) and to study stability and noise amplification of (41) we set  $\alpha = 1/L$  and  $\sigma = 1$  without loss of generality.

### A. Modal-decomposition

For the quadratic problem (3) with  $Q = Q^T \succ 0$ , we follow the approach of Section IV-A and utilize the eigenvalue decomposition of  $Q = V\Lambda V^T$  and the change of variables,  $\hat{x} := V^T(x - x^*)$ ,  $\hat{w} := V^T w$ , to bring (41) to,

$$\begin{aligned} \dot{\hat{\psi}}_i &= \hat{A}_i \hat{\psi}_i + \hat{B}_i \hat{w}_i, \\ \hat{z}_i &= \hat{C}_i \hat{\psi}_i \end{aligned} \quad (42a)$$

where  $\hat{w}_i$  is the  $i$ th component of the vector  $\hat{w}$ . For gradient flow dynamics (41a), we let  $\hat{\psi}_i := \hat{x}_i$ , which leads to

$$\hat{A}_i = -\alpha\lambda_i =: -a(\lambda_i), \hat{B}_i = 1, \hat{C}_i = 1. \quad (42b)$$

On the other hand, for accelerated gradient flow dynamics (41b),  $\hat{\psi}_i := [\hat{x}_i \ \hat{\dot{x}}_i]^T$ , and

$$\begin{aligned} \hat{A}_i &= \hat{A}(\lambda_i) := \begin{bmatrix} 0 & 1 \\ -a(\lambda_i) & -b(\lambda_i) \end{bmatrix} \\ \hat{B}_i &= [0 \ 1]^T, \hat{C}_i = [1 \ 0] \\ a(\lambda) &:= \alpha\lambda, \quad b(\lambda) := \theta + \gamma\alpha\lambda. \end{aligned} \quad (42c)$$

Even though functions  $a(\lambda)$  and  $b(\lambda)$  take different forms in continuous time, matrices  $\hat{A}_i$ ,  $\hat{B}_i$ , and  $\hat{C}_i$  in (42c) have the same structure as their discrete-time counterparts in (18).

### B. Optimal convergence rate

System (42) is stable if and only if the matrix  $\hat{A}_i$  is Hurwitz (i.e., if all of its eigenvalues have negative real parts). Moreover, the system is exponentially stable with the rate  $\rho$ ,

$$\|\hat{\psi}_i(\tau)\|_2 \leq c e^{-\rho\tau} \|\hat{\psi}_i(0)\|_2$$

if and only if the real parts of all eigenvalues of  $\hat{A}_i$  are less than or equal to  $-\rho$ . For gradient flow dynamics (41a) with  $\alpha = 1/L$ ,  $\hat{A}_i$ 's are real scalars and  $\rho$  is determined by

$$\rho_{\text{gfd}} := \min_i |\alpha\lambda_i| = m/L = 1/\kappa. \quad (43)$$

Note that  $\hat{A}_i$  in (42c) has the same structure as the matrix  $M$  in (20a). Lemma 5 is a continuous-time counterpart for Lemmas 1 and 2 and it provides conditions for (exponential) stability of matrices  $\hat{A}_i$  for accelerated gradient flow dynamics (41b).

*Lemma 5:* The real matrix  $M$  in (20a) satisfies

$$M \text{ is Hurwitz} \iff a, b > 0.$$

In addition, for any  $\rho > 0$ , we have

$$\max \{\Re(\text{eig}(M))\} \leq -\rho \iff \begin{cases} a \geq \rho(b - \rho) \\ b \geq 2\rho. \end{cases}$$

*Proof:* See Appendix E. ■

Conditions for stability and  $\rho$ -exponential stability in Lemma 5 respectively require inclusion of the point  $(b, a)$  to the open positive orthant and the  $\rho$ -parameterized cone shown in Figure 5. Furthermore, the normalization of the parameter  $\alpha$  to  $\alpha = 1/L$  yields the extra condition  $a \leq 1$ . For  $\rho < 1$ , combining this inequality with the exponential stability conditions in Lemma 5 further restricts the  $\rho$ -exponential stability cone to the triangle in the  $(b, a)$ -plane,

$$\Delta_\rho := \{(b, a) \mid b \geq 2\rho, \rho(b - \rho) \leq a \leq 1\} \quad (44a)$$

whose vertices are given by

$$X_\rho = (2\rho, \rho^2), \quad Y_\rho = (2\rho, 1), \quad Z_\rho = (\rho + 1/\rho, 1). \quad (44b)$$

For  $\rho = 1$ , the triangle  $\Delta_\rho$  is a single point and, for  $\rho > 1$ , adding the normalization condition  $a \leq 1$  makes the  $\rho$ -exponential stability conditions in Lemma 5 infeasible. Thus, in what follows, we confine our attention to  $\rho < 1$ .

Figure 5 illustrates the stability and  $\rho$ -exponential stability cones as well as the  $\rho$ -exponential stability triangle  $\Delta_\rho$ . The geometry of  $\Delta_\rho$  allows us to determine the largest condition number for which (41b) is  $\rho$ -exponentially stable.

*Proposition 5:* For a strongly convex quadratic objective function  $f \in \mathcal{Q}_m^L$  with the condition number  $\kappa = L/m$ , the optimal convergence rate and the corresponding parameters  $(\beta, \gamma)$  of accelerated gradient flow dynamics (41b) with  $\alpha = 1/L$  are

$$\rho = 1/\sqrt{\kappa}, \quad \beta = 1 + (v - 2)/\sqrt{\kappa}, \quad \gamma = v\sqrt{\kappa} \quad (45)$$



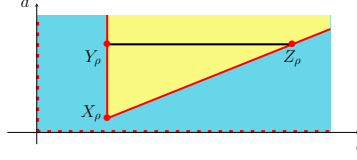


Figure 5. The open positive orthant (cyan) in the  $(b, a)$ -plane is the stability region for the matrix  $M$  in (20a). The intersections  $Y_\rho$  and  $Z_\rho$  of the stepsize normalization line  $a = 1$  (black) and the boundary of the  $\rho$ -exponential stability cone (yellow) established in Lemma 5, along with the cone apex  $X_\rho$  determine the vertices of the  $\rho$ -exponential stability triangle  $\Delta_\rho$  given by (44).

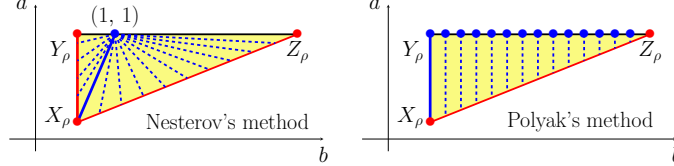


Figure 6. For a fixed  $\rho$ -exponential stability triangle  $\Delta_\rho$  (yellow) in (44), the line segments  $(b(\lambda), a(\lambda))$ ,  $\lambda \in [m, L]$  for Nesterov's accelerated ( $\gamma = \beta$ ) and the heavy-ball ( $\gamma = 0$ ) dynamics, as special examples of accelerated dynamics (41b) with constant parameters  $\gamma, \beta$ , and  $\alpha = 1/L$  are marked by dashed blue lines. The blue bullets correspond to the locus of the end point  $(b(L), a(L))$ , and the solid blue line segments correspond to the parameters for which the rate  $\rho$  is achieved for the largest possible condition number (45).

where  $v \in [0, 1]$ . This rate is achieved by the heavy-ball method ( $\gamma = 0$ ) with  $v = 0$  and, for  $\kappa \geq 4$ , by Nesterov's accelerated method ( $\gamma = \beta$ ) with  $v = (\sqrt{\kappa} - 2)/(\kappa - 1)$ .

*Proof:* See Appendix E. ■

Proposition 5 uses necessary and sufficient condition for  $\rho$ -exponential stability:  $(b(\lambda), a(\lambda)) \in \Delta_\rho$  for every  $\lambda \in [m, L]$ . Figure 6 illustrates the orientation of this line segment in  $\Delta_\rho$  for the heavy-ball and Nesterov's algorithms. For the optimal values of parameters, Proposition 5 implies that accelerated gradient flow dynamics (41b) reduces the settling time  $1/\rho$  relative to gradient flow dynamics (41a) by a factor of  $\sqrt{\kappa}$ , i.e.,

$$\rho_{\text{agd}}/\rho_{\text{gfd}} = \sqrt{\kappa}.$$

### C. Noise amplification

Similar to the discrete-time setting, exponentially stable LTI systems in (42) driven by white noise reach a statistical steady-state with  $\lim_{t \rightarrow \infty} \mathbb{E}(\hat{\psi}_i(t)) = 0$ . Furthermore, the variance

$$J := \lim_{t \rightarrow \infty} \frac{1}{t} \int_0^t \mathbb{E}(\|x(\tau) - x^*\|_2^2) d\tau \quad (46)$$

can be computed from the solution of the *continuous-time algebraic Lyapunov equation* [42]. The following theorem provides analytical expressions for the steady-state variance  $J$ .

*Theorem 6:* For a strongly convex quadratic objective function  $f \in \mathcal{Q}_m^L$  with Hessian  $Q$ , the noise amplification  $J$  of (41) with any constant stabilizing parameters  $(\alpha, \beta, \gamma)$  is determined by  $J = \sum_{i=1}^n \hat{J}(\lambda_i)$ . Here,  $\hat{J}(\lambda_i)$  is the modal contribution of the  $i$ th eigenvalue  $\lambda_i$  of  $Q$  to the noise amplification

$$\hat{J}_{\text{gfd}}(\lambda) = 1/(2a(\lambda)), \quad \hat{J}_{\text{agd}}(\lambda) = 1/(2a(\lambda)b(\lambda))$$

where the functions  $a$  and  $b$  are given by (42c).

We omit the proof of Theorem 6 as it uses similar arguments to those used in the proof of [30, Theorem 1].

For  $\alpha = 1/L$  and the parameters that optimize the convergence rate provided by Proposition 5, we can use the explicit forms of  $\hat{J}(\lambda)$  established in Theorem 6 to obtain

$$J_{\text{max}} = \begin{cases} ((n-1)\kappa + 1)/2 & \text{gfd} \\ ((n-1)\kappa\sqrt{\kappa} + \sqrt{\kappa})/4 & \text{agd (hb)} \\ ((n-1)\kappa\sqrt{\kappa} + 2)/4 & \text{agd (na)} \end{cases} \quad J_{\text{min}} = \begin{cases} (\kappa + (n-1))/2 & \text{gfd} \\ (\kappa\sqrt{\kappa} + (n-1)\sqrt{\kappa})/4 & \text{agd (hb)} \\ (\kappa\sqrt{\kappa} + (n-1)2)/4 & \text{agd (na)} \end{cases} \quad (47)$$

For all three cases, the largest noise amplification  $J_{\text{max}}$  occurs when the Hessian matrix  $Q$  has  $n-1$  eigenvalues at  $\lambda = L$  and one at  $\lambda = m$ , and the smallest noise amplification  $J_{\text{min}}$  occurs when  $Q$  has  $n-1$  eigenvalues at  $\lambda = m$  and one at  $\lambda = L$ . Despite the  $\sqrt{\kappa}$  improvement in the convergence rate achieved by the accelerated gradient

flow dynamics, the corresponding  $J_{\max}$  and  $J_{\min}$  are larger than those of gradient flow dynamics by a factor of  $\sqrt{\kappa}$ . We next generalize this result to any stabilizing  $(\beta, \gamma)$  and establish similar trends for all  $f \in \mathcal{Q}_m^L$ .

#### D. Convergence and noise amplification tradeoffs

The next result is the continuous-time analogue of Theorem 2 and it establishes a lower bound on the product of the noise amplification and the settling time  $T_s = 1/\rho$  of the accelerated gradient flow dynamics for any  $(\beta, \gamma)$ .

*Theorem 7:* Let the parameters  $(\beta, \gamma)$  be such that the accelerated gradient flow dynamics (41b) with  $\alpha = 1/L$  is exponentially stable with rate  $\rho = 1/T_s$  for all  $f \in \mathcal{Q}_m^L$ . Then,  $J_{\max}$  and  $J_{\min}$  in (10) satisfy,

$$J_{\max} \times T_s \geq (n-1) \frac{\kappa^2}{4} + \frac{1}{2(1+\rho^2)} \quad (48a)$$

$$J_{\min} \times T_s \geq \frac{\kappa^2}{4} + \frac{(n-1)}{2(1+\rho^2)}. \quad (48b)$$

*Proof:* See Appendix E. ■

Theorem 7 demonstrates that the tradeoff between  $J_{\max}$  and  $J_{\min}$  and the settling time established in Theorem 2 for the two-step momentum algorithm extends to the continuous-time dynamics. For a fixed problem size  $n$  and the parameters that optimize the convergence rate provided in Lemma 5, we can use (47) to conclude that the bounds in Theorem 7 are order-wise tight for the parameters that achieve the optimal convergence rate.

## VII. PROOFS OF THEOREMS 1-4

### A. Proof of Theorem 1

From Theorem 5 it follows that we can use upper bounds on  $\hat{J}(\lambda)$  over  $\lambda \in [m, L]$  to establish an upper bound on  $J$ . Since the algorithm achieves the convergence rate  $\rho$ , combining equation (19) and Lemma 2 yield  $(b(\lambda), a(\lambda)) \in \Delta_\rho$  for all  $\lambda \in [m, L]$ . As we demonstrate in Appendix B, the function  $\hat{J}$  is convex in  $(b, a)$  over the stability triangle  $\Delta$ . In addition,  $\Delta_\rho \subset \Delta$  is the convex hull of the points  $X_\rho, Y_\rho, Z_\rho$  in the  $(b, a)$ -plane. Since the maximum of a convex function over the convex hull of a finite set of points is attained at one of these points,  $\hat{J}$  attains its maximum over  $\Delta_\rho$  at  $X_\rho, Y_\rho$ , or  $Z_\rho$ .

Using the definition of  $X_\rho, Y_\rho$ , and  $Z_\rho$  in (22c), the affine relations (29), and the analytical expression for  $\hat{J}$  in Theorem 5, it follows that the maximum occurs at vertices  $X_\rho$  and  $Y_\rho$ ,

$$\hat{J}_{\max} := \max_{\lambda \in [m, L]} \hat{J}(\lambda) = \frac{\sigma_w^2(1+\rho^2)}{(1-\rho)^3(1+\rho)^3}$$

where we use  $d_{X_\rho} = l_{Y_\rho} = (1-\rho)^2$ ,  $l_{X_\rho} = d_{Y_\rho} = (1+\rho)^2$ , and  $h_{X_\rho} = h_{Y_\rho} = 1-\rho^2$ . Combining the above identity with Theorem 5 completes the proof of (12a).

We use an argument similar to the proof of Proposition 1 to prove (12b). In particular, since  $(b(L), a(L)) \in \Delta_\rho$ , we have

$$\alpha L = d(L) \leq d_{\max} = (1+\rho)^2$$

where  $d$  given by (24) is the horizontal signed distance to the edge  $XZ$  of the stability triangle  $\Delta$ . On the other hand,  $d_{\max}$  is the largest value that  $d$  can take among all points  $(b, a) \in \Delta_\rho$  and it corresponds to the vertex  $Y_\rho$ ; see equation (26a). Combining this inequality with  $\sigma_w = \alpha\sigma$  and (12a) completes the proof of Theorem 1.

### B. Proof of Theorem 2

Using the expression  $J = \sum_i \hat{J}(\lambda_i)$  established in Theorem 5, we have the decomposition

$$J = \hat{J}(m) + \sum_{i=1}^{n-1} \hat{J}(\lambda_i). \quad (49)$$

To prove the lower bounds (13b) and (13d) on  $J_{\min} \times T_s$ , we establish a lower bound on  $\hat{J}(m) \times T_s$  that scales quadratically with  $\kappa$ , and a general lower bound on  $\hat{J}(\lambda) \times T_s$ .

Case  $\sigma_w = \sigma$ : The proof of (13b) utilizes the following inequalities

$$\frac{\hat{J}(m)}{1-\rho} \geq \frac{\sigma_w^2 \kappa^2}{2(1+\rho)^5} \quad (50a)$$

$$\frac{\hat{J}(\lambda)}{1-\rho} \geq \frac{\sigma_w^2(\sqrt{\kappa}+1)}{2}. \quad (50b)$$

We first prove (50a). Our approach builds on the proof of Proposition 1. In particular,  $d(\lambda) = \alpha\lambda$  for the point  $(b(\lambda), a(\lambda))$ , where  $d$  and  $(b, a)$  are defined in (29) and (18c), respectively. Thus,  $d(m) = d(L)/\kappa$ . Furthermore, Lemma 3 implies  $(b(\lambda), a(\lambda)) \in \Delta_\rho$  for  $\lambda \in [m, L]$ . Thus, the trivial inequality  $d(L) \leq d_{\max}$  leads to

$$d(m) \leq d_{\max}/\kappa = (1+\rho)^2/\kappa \quad (51)$$

where  $d_{\max} = (1+\rho)^2$  is the largest value that  $d$  can take among all points  $(b, a) \in \Delta_\rho$ ; see equation (26a). We now use Theorem 5 to write

$$\frac{\hat{J}(\lambda)}{1-\rho} = \frac{\sigma_w^2(d(\lambda) + l(\lambda))}{2d(\lambda)h(\lambda)l(\lambda)(1-\rho)} \geq \frac{\sigma_w^2}{2d(\lambda)h(\lambda)(1-\rho)}. \quad (52)$$

Next, we lower bound the right-hand side of (52). Let  $\mathcal{L}$  be the line that passes through  $(b(\lambda), a(\lambda))$  which is parallel to the edge  $XZ$  of the stability triangle  $\Delta$ , and let  $G$  be the intersection of  $\mathcal{L}$  and the edge  $X_\rho Z_\rho$  of the  $\rho$ -stability triangle  $\Delta_\rho$ ; see Figure 7 for an illustration. It is easy to verify that

$$h_G \geq h(\lambda), \quad d_G = d(\lambda) \quad (53a)$$

where  $h_G$  and  $d_G$  correspond to the values of  $h$  and  $d$  associated with the point  $G$ . In addition, since  $G$  lies on the edge  $X_\rho Z_\rho$ ,  $h_G$  and  $d_G$  satisfy the affine relation

$$h_G = 1 - \rho + d_G \rho / (1 - \rho). \quad (53b)$$

This follows from the equation of the line  $X_\rho Z_\rho$  in the  $(b, a)$ -plane and from the definitions of  $d$  and  $h$  in (29). Furthermore, combining (53a) and (53b) implies

$$\frac{\sigma_w^2}{2d(\lambda)h(\lambda)(1-\rho)} \stackrel{(a)}{\geq} \frac{\sigma_w^2}{2d(\lambda)h_G(1-\rho)} \stackrel{(b)}{=} \frac{\sigma_w^2}{2d(\lambda)((1-\rho)^2 + \rho d(\lambda))}. \quad (54a)$$

For  $\lambda = m$ , we can further write

$$\frac{\sigma_w^2}{2d(m)((1-\rho)^2 + \rho d(m))} \geq \frac{\sigma_w^2}{2 \frac{(1+\rho)^2}{\kappa} \left( \frac{(1+\rho)^2}{\kappa} + \rho \frac{(1+\rho)^2}{\kappa} \right)} = \frac{\sigma_w^2 \kappa^2}{2(1+\rho)^5} \quad (54b)$$

where the inequality is obtained from (27) and (51). Combining (52), (54a), and (54b) completes the proof of (50a).

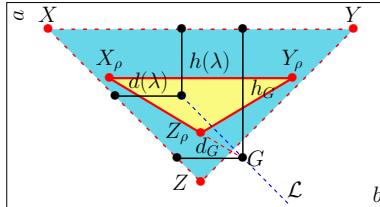


Figure 7. The line  $\mathcal{L}$  (blue, dashed) and the intersection point  $G$ , along with the distances  $d_1$ ,  $h_1$ ,  $d_G$ , and  $h_G$  as introduced in the proof of Theorem 2.

Next, we prove the general lower bound in (50b). As we demonstrate in Appendix B, the modal contribution  $\hat{J}$  to the noise amplification is a convex function of  $(b, a)$  which takes its minimum  $\hat{J}_{\min} = \sigma_w^2$  over the stability triangle  $\Delta$  at the origin  $b = a = 0$ . Combining this fact with the lower bound in (7) on  $\rho$  completes the proof of (50b).

Finally, we can obtain the lower bound (13b) on  $J_{\min} \times T_s$  by combining (49) and (50).

Case  $\sigma_w = \alpha\sigma$ : The proof of (13d) utilizes the following inequalities

$$\frac{\hat{J}(\lambda)}{1-\rho} \geq \frac{\sigma^2}{2\lambda^2(1+\rho)} \quad (55a)$$

$$\frac{\hat{J}(\lambda)}{1-\rho} \geq \frac{\sigma^2(1-\rho)^3\kappa^2}{L^2}. \quad (55b)$$

In particular, (13d) follows from using (55a) for  $\lambda = m$  and taking the maximum of (55a) and (55b) for the other eigenvalues to bound the expression for  $J$  established by Theorem 5.

We first prove (55a). By combining (52) and (54a), we obtain

$$\frac{\hat{J}(\lambda)}{1-\rho} \geq \frac{\alpha^2\sigma^2}{2d(\lambda)((1-\rho)^2 + \rho d(\lambda))}. \quad (56)$$

Since  $d(\lambda) \geq d_{\min} := (1-\rho)^2$ , where  $d_{\min}$  is the smallest value of  $d$  over  $\Delta_\rho$ , [cf. (26b)], we can write

$$\frac{\alpha^2\sigma^2}{2d(\lambda)((1-\rho)^2 + \rho d(\lambda))} \geq \frac{\alpha^2\sigma^2}{2d(\lambda)^2(1+\rho)} = \frac{\sigma^2}{2\lambda^2(1+\rho)}. \quad (57)$$

Combining (56) and (57) completes the proof of (55a).

To prove (55b) we use  $d(\lambda) \geq d_{\min} := (1-\rho)^2$  and  $d(m) = \alpha m$ , to obtain  $\alpha \geq (1-\rho)^2\kappa/L$ . Combining this inequality with  $\hat{J}_{\min} = \sigma_w^2 = \alpha^2\sigma^2$  yields (55b). Finally, we obtain the lower bound (13d) on  $J_{\min} \times T_s$  by combining (49) and (55).

To obtain the lower bounds (13a) and (13c) on  $J_{\max} \times T_s$ , we consider a quadratic function for which the Hessian has  $n-1$  eigenvalues at  $\lambda = m$  and one eigenvalue at  $\lambda = L$ . For such a function, we can use Theorem 5 to write

$$J_{\max} \geq J = (n-1)\hat{J}(m) + \hat{J}(L). \quad (58)$$

Case  $\sigma_w = \sigma$ : To prove (13a), we use inequalities in (50a) and (50b) to bound  $\hat{J}(m)/(1-\rho)$  and  $\hat{J}(L)/(1-\rho)$  in (58), respectively.

Case  $\sigma_w = \alpha\sigma$ : To prove (13c), we use inequality in (55a) with  $\lambda = m$  to lower bound  $\hat{J}(m)/(1-\rho)$ , and combine (55a) and (55b) to lower bound  $\hat{J}(L)/(1-\rho)$  in (58). This completes the proof.

### C. Proof of Theorem 3

As described in Section V, the parameters in Theorem 3 are obtained by placing the end points of the horizontal line segment  $(b(\lambda), a(\lambda))$  parameterized by  $\lambda \in [m, L]$  at the edges  $X_\rho Z_\rho$  and  $Y_\rho Z_\rho$  of the  $\rho$ -linear convergence triangle  $\Delta_\rho$ . These parameters can be equivalently represented by (32) where the scalar  $c$  given in Lemma 4 satisfies  $c \geq 0$  if and only if  $T_s \leq (\kappa+1)/2$ . The proof of Theorem 3 follows from combining Lemma 4 and Proposition 2.

### D. Proof of Theorem 4

The following proposition allows us to prove the lower bounds in Theorem 4.

*Proposition 6:* Let  $\rho = \rho(A) = 1 - 1/T_s$  be the convergence rate of the two-step momentum algorithm (2). Then, the largest and smallest modal contributions to noise amplification given by (31b) satisfy

$$\hat{J}_{\max} \geq \frac{\sigma_w^2}{2(1+\rho)^2} T_s, \quad \hat{J}_{\min} \geq \sigma_w^2.$$

*Proof:* The inequality  $\hat{J}_{\min} \geq \sigma_w^2$  follows from the fact that  $\hat{J}$ , as a function of  $(b, a)$ , takes its minimum value at the origin; see Appendix B. The proof for  $\hat{J}_{\max}$  utilizes the fact that for any constant parameters  $(\alpha, \beta, \gamma)$  and fixed condition number, the spectral radius  $\rho(A)$  corresponds to the smallest  $\rho$ -linear convergence triangle  $\Delta_\rho$  that contains the line segment  $(b(\lambda), a(\lambda))$  for  $\lambda \in [m, L]$ . Thus, at least one of the end points  $(b(m), a(m))$  or  $(b(L), a(L))$  will be on the boundary of the triangle  $\Delta_{\rho(A)}$ . Combining this with the fact that  $d(m) \leq d(L)$ , it follows that at least one of the following holds

$$\begin{aligned} (b(m), a(m)) &\in X_\rho Z_\rho \text{ or } X_\rho Y_\rho, \\ (b(L), a(L)) &\in Y_\rho Z_\rho \text{ or } X_\rho Y_\rho. \end{aligned}$$

Together with the concrete values of vertices (21c) in terms of  $\rho$ , this yields

$$1 - \rho \geq \min \{h(m), h(L), l(L)/(1 + \rho), d(m)/(1 + \rho)\} \quad (59)$$

Also, using Theorem 5 and noting that the maximum values that  $h(\lambda)$ ,  $d(\lambda)$ , and  $l(\lambda)$  can take among  $\Delta_\rho$  are given by  $1 + \rho^2$ ,  $(1 + \rho)^2$ , and  $(1 + \rho)^2$ , respectively, we can write

$$\begin{aligned} \hat{J}(m) &\geq \frac{\sigma_w^2}{2h(m)d(m)} \geq \max \left\{ \frac{\sigma_w^2}{2h(m)(1 + \rho)^2}, \frac{\sigma_w^2}{2d(m)(1 + \rho)^2} \right\} \\ \hat{J}(L) &\geq \frac{\sigma_w^2}{2h(L)l(L)} \geq \max \left\{ \frac{\sigma_w^2}{2h(L)(1 + \rho)^2}, \frac{\sigma_w^2}{2l(L)(1 + \rho)^2} \right\}. \end{aligned} \quad (60)$$

Finally, by the convexity of  $\hat{J}$  (see Appendix B), we have  $\hat{J}_{\max} \geq \max\{\hat{J}(m), \hat{J}(L)\}$ . Combining this with (59) and (60) completes the proof.  $\blacksquare$

The lower bounds in Theorem 4 follow from combining Proposition 6 with the expression for  $J$  in Theorem 5. To obtain the upper bounds, we note that the parameter  $c$  in Lemma 4 satisfies  $c \in [-1, 0]$  if and only if  $T_s \geq (\kappa + 1)/2$ . Thus, we can use Proposition 3 to complete the proof.

## VIII. CONCLUDING REMARKS

We have examined the amplification of stochastic disturbances for a class of two-step momentum algorithms in which the iterates are perturbed by an additive white noise which arises from uncertainties in gradient evaluation or in computing the iterates. For both noise models, we establish lower bounds on the product of the settling time and the smallest/largest steady-state variance of the error in the optimization variable. These bounds scale with  $\kappa^2$  for all stabilizing parameters, which reveals a fundamental limitation imposed by the condition number  $\kappa$  in designing algorithms that tradeoff noise amplification and convergence rate. In addition, we provide a novel geometric viewpoint of stability and  $\rho$ -linear convergence. This viewpoint brings insight into the relation between noise amplification, convergence rate, and algorithmic parameters. It also allows us to (i) take an alternative approach to optimizing convergence rates for standard algorithms; (ii) identify key similarities and differences between the iterate and gradient noise models; and (iii) introduce parameterized families of algorithms for which the parameters can be continuously adjusted to tradeoff noise amplification and settling time. By utilizing positive and negative momentum parameters in accelerated and decelerated regimes, respectively, we demonstrate that a parameterized family of the heavy-ball-like algorithms can achieve order-wise Pareto optimality for all settling times and both noise models. We also extend our analysis to continuous-time dynamical systems that can be discretized via an implicit-explicit Euler scheme to obtain the two-step momentum algorithm. For such gradient flow dynamics, we show that similar fundamental stochastic performance limitations hold as in discrete time.

Our ongoing work focuses on extending these results to algorithms with more complex structures including update strategies that utilize information from more than the last two iterates and time-varying algorithmic parameters [44]. It is also of interest to identify fundamental performance limitations of stochastic gradient descent algorithms in which both additive and multiplicative stochastic disturbances exist [45], [46].

## ACKNOWLEDGMENTS

We thank Laurent Lessard for his comments on an earlier draft of this manuscript.

## APPENDIX

### A. Settling time

If  $\rho$  denotes the linear convergence rate,  $T_s = 1/(1 - \rho)$  quantifies the *settling time*. The inequality in (5) shows that  $c\rho^t \leq \epsilon$  provides a sufficient condition for reaching the accuracy level  $\epsilon$  with  $\|\psi^t\|_2/\|\psi^0\|_2 \leq \epsilon$ . Taking the logarithm of  $c\rho^t \leq \epsilon$  and using the first-order Taylor series approximation  $\log(1 - x) \approx -x$  around  $x = 0$  yields a sufficient condition on the number of iterations  $t$  for an algorithm to reach  $\epsilon$ -accuracy,

$$t \geq \log(\epsilon/c)/\log(1 - 1/T_s) \approx T_s \log(c/\epsilon).$$

In continuous time, the sufficient condition for reaching  $\epsilon$ -accuracy  $ce^{-\rho t} \leq \epsilon$  yields  $t \geq \log(c/\epsilon)/\rho$ , and  $T_s = 1/\rho$  can be used to assess the settling time.

### B. Convexity of modal contribution $\hat{J}$ to noise amplification

To show the convexity of  $\hat{J}$ , we use the fact that the function  $g(x) = \prod_{i=1}^d x_i^{-1}$  is convex over the positive orthant  $\mathbb{R}_{++}^d$ . This can be verified by noting that its Hessian satisfies

$$\nabla^2 g(x) = g(x) (\text{diag}(x) + xx^T) \succ 0$$

where  $\text{diag}(\cdot)$  is the diagonal matrix. By Theorem 5, we have

$$\frac{\hat{J}}{\sigma_w^2} = \frac{d+l}{2dhl} = \frac{1}{2hd} + \frac{1}{2hl}$$

where we have dropped the dependence on  $\lambda$  for simplicity. The functions  $1/(2hd)$  and  $1/(2hl)$  are both convex over the positive orthant  $d, h, l > 0$ . Thus,  $\hat{J}$  is convex with respect to  $(d, h, l)$ . In addition, since  $d, h$ , and  $l$  are all affine functions of  $a$  and  $b$ , we can use the equivalence relation in (30a) to conclude that  $\hat{J}$  is also convex in  $(b, a)$  over the stability triangle  $\Delta$ . Finally, since  $b(\lambda)$  and  $a(\lambda)$  are affine in  $\lambda$ , it follows that for any stabilizing parameters,  $\hat{J}$  is also convex with respect to  $\lambda$  over the interval  $[m, L]$ .

Convexity of  $\hat{J}$  allows us to use first-order conditions to find its minimizer. In particular, since for  $\sigma_w = 1$

$$\begin{aligned} \frac{\partial \hat{J}}{\partial d} &= -\frac{1}{2hd^2}, & \frac{\partial \hat{J}}{\partial l} &= -\frac{1}{2hl^2}, & \frac{\partial \hat{J}}{\partial h} &= -\frac{l+d}{2h^2dl} \\ \frac{\partial d}{\partial a} &= \frac{\partial l}{\partial a} = -\frac{\partial h}{\partial a} = \frac{\partial d}{\partial b} = -\frac{\partial l}{\partial b} = 1, & \frac{\partial h}{\partial b} &= 0 \end{aligned}$$

it is easy to verify that  $\partial \hat{J} / \partial a = \partial \hat{J} / \partial b = 0$  at  $a = b = 0$ . Thus,  $\hat{J}$  takes its minimum  $\hat{J}_{\min} = \sigma_w^2$  over the stability triangle  $\Delta$  at  $a = b = 0$ , which corresponds to  $d = h = l = 1$ .

### C. Proofs of Section IV

1) *Proof of Lemma 2:* We start by noting that  $\rho(M) \leq \rho$  if and only if  $\rho(M') \leq 1$  where  $M' := M/\rho$ . The characteristic polynomial associated with  $M'$ ,  $F_{\rho}(z) = z^2 + (b/\rho)z + a/\rho^2$ , allows us to use similar arguments to those presented in the proof of Lemma 1 to show that

$$\rho(M') \leq 1 \iff (b/\rho, a/\rho^2) \in \Delta_1 \quad (61)$$

where  $\Delta_1 := \{(b, a) \mid |b| - 1 \leq a \leq 1\}$  is the closure of the set  $\Delta$  in (21b). Finally, the condition on the right-hand side of (61) is equivalent to  $(b, a) \in \Delta_{\rho}$ , where  $\Delta_{\rho}$  is given by (22b).

*Remark 6:* The eigenvalues of the matrix  $M$  in (20a) are given by  $(-b \pm \sqrt{b^2 - 4a})/2$ , and the sign of  $b^2 - 4a$  determines if the eigenvalues are real or complex. The condition  $a = b^2/4$  defines a parabola that passes through the vertices  $X_{\rho} = (-2\rho, \rho^2)$  and  $Y_{\rho} = (2\rho, \rho^2)$  of the triangle  $\Delta_{\rho}$  and is tangent to the edges  $X_{\rho}Z_{\rho}$  and  $Y_{\rho}Z_{\rho}$  for all  $\rho < 1$ ; see Figure 8. For the optimal values of parameters provided in Table I, we can combine this observation and the information in Figure 3 to conclude that while all eigenvalues of the matrix  $A$  in (4a) are real for gradient descent, they can be both real and complex for Nesterov's accelerated algorithm, and they come in complex-conjugate pairs for heavy-ball method.

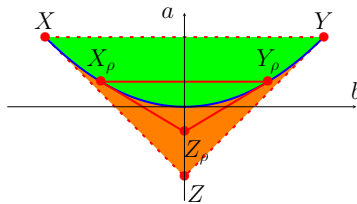


Figure 8. The green and orange subsets of the stability triangle  $\Delta$  (dashed-red) correspond to complex conjugate and real eigenvalues for the matrix  $M$  in (20a), respectively. The blue parabola  $a = b^2/4$  corresponds to the matrix  $M$  with repeated eigenvalues and it is tangent to the edges  $X_{\rho}Z_{\rho}$  and  $Y_{\rho}Z_{\rho}$  of the  $\rho$ -linear convergence triangle  $\Delta_{\rho}$  (solid red).

2) *Proof of Equation (28c):* According to Figure 3, in order to find the largest ratio  $d(L)/d(m)$  over the  $\rho$ -linear convergence set  $\Delta_{\rho}$  for Nesterov's accelerated method, we need to check the pairs of points  $\{E, E'\}$  that lie on the boundary of the triangle  $\Delta_{\rho}$ , whose line segment  $EE'$  passes through the origin  $O$ . If one of the end points  $E$

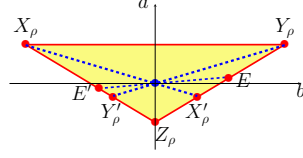


Figure 9. The points  $X'_\rho$  and  $Y'_\rho$  as defined in (62) along with an arbitrary line segment  $EE'$  passing through the origin in the  $(b, a)$ -plane.

lies on the edge  $X_\rho Y_\rho$ , then depending on whether the other end point  $E'$  lies on the edge  $X_\rho Z_\rho$  or  $Y_\rho Z_\rho$ , we can continuously increase the ratio  $d_E/d_{E'}$  by moving  $E$  toward the vertices  $Y_\rho$  or  $X_\rho$ , respectively. Thus, this case reduces to checking only the ratio  $d_E/d_{E'}$  for the line segments  $X_\rho X'_\rho$  and  $Y_\rho Y'_\rho$ , where

$$X'_\rho = (2\rho/3, -\rho^2/3), \quad Y'_\rho = (-2\rho/3, -\rho^2/3) \quad (62)$$

are the intersections of  $OX_\rho$  with  $Y_\rho Z_\rho$ , and  $OY_\rho$  with  $X_\rho Z_\rho$ ; see Figure 9. Regarding the case when neither  $E$  nor  $E'$  lies on the edge  $X_\rho Y_\rho$ , let us assume without loss of generality that  $E$  and  $E'$  lie on  $Y_\rho Z_\rho$  and  $X_\rho Z_\rho$ , respectively. In this case, we can parameterize the ratio using

$$\frac{d_E}{d_{E'}} = \frac{(1+c)(1/(1-\rho)-c)}{(1-c)(1/(1+\rho)+c)}, \quad c \in [-1/2, 1/2] \quad (63)$$

where  $c\rho$  determines the slope of  $EE'$ . The general shape of this function is provided in Figure 10. It is easy to verify that  $d_E/d_{E'}$  takes its maximum over  $c \in [-1/2, 1/2]$  at one of the boundaries. Thus, this case also reduces to checking only the ratio  $d_E/d_{E'}$  for the line segments  $X_\rho X'_\rho$  and  $Y_\rho Y'_\rho$ . We complete the proof by noting that

$$\frac{d_{X'_\rho}}{d_{X_\rho}} = \frac{(1+\rho)(3-\rho)}{3(1-\rho)^2}, \quad \frac{d_{Y'_\rho}}{d_{Y_\rho}} = \frac{3(1+\rho)^2}{(3+\rho)(1-\rho)}$$

satisfy  $d_{X'_\rho}/d_{X_\rho} > d_{Y'_\rho}/d_{Y_\rho}$ .

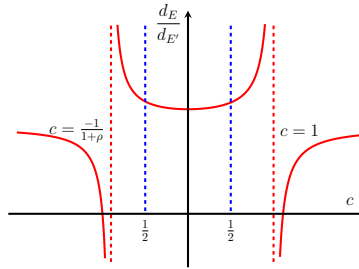


Figure 10. The ratio  $d_E/d_{E'}$  in (63) for Nesterov's method, where  $E$  and  $E'$  lie on the edges  $Y_\rho Z_\rho$  and  $X_\rho Z_\rho$  of the  $\rho$ -linear convergence triangle  $\Delta_\rho$ , and  $c\rho$  determines the slope of  $EE'$  which passes through the origin.

#### D. Proofs of Section V

1) *Proof of Lemma 4:* We show that the parameters  $(\alpha, \beta, \gamma)$  in (32) place the points  $(b(m), a(m))$  and  $(b(L), a(L))$  on the edges  $X_\rho Z_\rho$  and  $Y_\rho Z_\rho$  of the  $\rho$ -linear convergence triangle  $\Delta_\rho$ , respectively. In particular, we can use a scalar  $c \in [-1, 1]$  to parameterize the end points as

$$(b(m), a(m)) = (-(1+c)\rho, c\rho^2), \quad (b(L), a(L)) = ((1+c)\rho, c\rho^2).$$

Using the definition of  $a$  and  $b$  in (18c), we can solve the above equations for  $(\alpha, \beta, \gamma)$  to verify the desired parameters. Thus, the algorithm achieves the convergence rate  $\rho$ . In addition the points  $c = 0$  and  $c = 1$  recover gradient descent and heavy-ball method with the parameters that optimize the convergence rate; see Table I.

Furthermore,  $h$ ,  $d$ , and  $l$  in (29) are given by

$$\begin{aligned} h(m) &= h(L) = 1 - c\rho^2 \\ d(m) &= l(L) = (1-\rho)(1-c\rho) \\ l(m) &= d(L) = (1+\rho)(1+c\rho) \end{aligned} \quad (64a)$$

and the condition number is determined by

$$\kappa = \frac{\alpha L}{\alpha m} = \frac{d(L)}{d(m)} = \frac{l(m)}{d(m)}. \quad (64b)$$

Combining (64b) with (64a), and rearranging terms yields the desired expression for  $c$  in terms of  $\rho$  and  $\kappa$ .

The analytical expressions in Theorem 5 imply that for the parameters in (32), the function  $\hat{J}(\lambda)$  is symmetric over  $[m, L]$ , i.e.,  $\hat{J}(\lambda) = \hat{J}(m + L - \lambda)$  for all  $\lambda \in [m, L]$ . In addition, as we demonstrate in Appendix B,  $\hat{J}(\lambda)$  is convex. Thus,  $\hat{J}(\lambda)$  attains its maximum at  $\lambda = m$  and  $\lambda = L$  and we can use the expression for  $\hat{J}(\lambda)$  in Theorem 5 to obtain the maximum value,

$$\hat{J}(m) = \frac{\sigma_w^2(d(m) + l(m))}{2h(m)d(m)l(m)} = \frac{\sigma_w^2(\kappa + 1)}{2h(m)l(m)} \quad (64c)$$

where the second equality follows from (64b). Combining (64a) and (64c) yields the expression for  $\hat{J}(m)$ .

Also, symmetry and convexity imply that  $\hat{J}(\lambda)$  attains its minimum at the midpoint  $\lambda = \hat{\lambda} := (m + L)/2 = (1 + \beta)/\alpha$ . This point corresponds to  $(b(\hat{\lambda}), a(\hat{\lambda})) = (0, c\rho^2)$  in the  $(b, a)$ -plane and it thus satisfies

$$h(\hat{\lambda}) = 1 - c\rho^2, \quad d(\hat{\lambda}) = l(\hat{\lambda}) = 1 + c\rho^2. \quad (64d)$$

Using (64d) to evaluate the expression for  $\hat{J}(\lambda)$  at the point  $\lambda = \hat{\lambda}$  yields the desired minimum value.

2) *Proof of Proposition 2:* Using the expressions established in Lemma 4, it is straightforward to verify that

$$\begin{aligned} \hat{J}(m) \times T_s &= \sigma_w^2 p_{1c}(\rho) \kappa(\kappa + 1) \\ \hat{J}(\hat{\lambda}) \times T_s &= \sigma_w^2 \kappa p_{2c}(\rho) \end{aligned}$$

and that, for the gradient noise model ( $\sigma_w = \alpha\sigma$ ), we have

$$\begin{aligned} \hat{J}(m) \times T_s &= \sigma^2 p_{3c}(\rho) \kappa(\kappa + 1) \\ \hat{J}(\hat{\lambda}) &= \sigma^2 \kappa p_{2c}(\rho) \end{aligned}$$

where the functions  $p_{1c}(\rho)$ - $p_{4c}(\rho)$  are given by (36). Thus, the expressions for  $J_{\max}$  and  $J_{\min}$  follow from Corollary 2. The bounds on  $p_{1c}(\rho)$ - $p_{4c}(\rho)$  follow from the fact that, for  $\rho \in (0, 1)$ , we have

$$q_c(\rho) = \frac{1 - c\rho}{1 - c\rho^2} \in \begin{cases} [1/(1 + c\rho), 1] & c \in [0, 1] \\ [1/2, 2] & c \in [-1, 0]. \end{cases}$$

This completes the proof.

3) *Proof of Proposition 3:* Using the expressions established in Lemma 4, it is straightforward to verify that

$$\begin{aligned} \hat{J}(m) &= \sigma_w^2 p_{5c}(\rho) (1 + 1/\kappa) T_s \\ \hat{J}(\hat{\lambda}) &= \sigma_w^2 p_{6c}(\rho) T_s / \kappa \end{aligned}$$

where  $p_{5c}$  and  $p_{6c}$  are given by Proposition 3. Thus, the expressions for  $J_{\max}$  and  $J_{\min}$  follow from Corollary 2. The bounds on  $p_{5c}$  and  $p_{6c}$  also follow from  $c \in [-1, 0]$  and  $\rho \in (0, 1)$ .

4) *Proof of Proposition 4:* We show that  $(\alpha, \beta, \gamma)$  correspond to the parameterized family of Nesterov-like algorithms in which the end points of the line segment  $(b(\lambda), a(\lambda))$ ,  $\lambda \in [m, L]$ , lie on the edges  $X_\rho Z_\rho$  and  $Y_\rho Z_\rho$  of the  $\rho$ -linear convergence triangle  $\Delta_\rho$ . In particular, we can use a scalar  $c \in [0, 1/2]$  to parameterize the lines passing through the origin via  $a = -c\rho b$ . This yields

$$\begin{aligned} (b(m), a(m)) &= (-\rho/(1 - c), c\rho^2/(1 - c)) \\ (b(L), a(L)) &= (\rho/(1 + c), -c\rho^2/(1 + c)). \end{aligned}$$

Using the definitions of  $a$  and  $b$  in (18c), we can solve the above equations for  $(\alpha, \beta, \gamma)$  to verify the desired parameters. Thus, the algorithm achieves the convergence rate  $\rho$  and the extreme points  $c = 0$  and  $c = 1/2$  recover gradient descent and Nesterov's method with the parameters provided in Table I that optimize settling times.

In Lemma 6, we establish expressions for the convergence rate and largest/smallest modal contributions to noise amplification in terms of the condition number for this family of parameters.

*Lemma 6:* For the class of functions  $\mathcal{Q}_m^L$  with condition number  $\kappa = L/m$ , the extreme values  $\hat{J}_{\max}$  and  $\hat{J}_{\min}$



of  $\hat{J}(\lambda)$  over  $[m, L]$  associated with the two-step momentum algorithm in (2) with parameters (38) satisfy

$$\begin{aligned} \hat{J}_{\max} &= \hat{J}(m) = \frac{\sigma_w^2(1-c)^2(r\kappa+1)}{2(1-c-c\rho^2)(1+\rho)(1-c+c\rho)} \\ &\geq \hat{J}(L) = \frac{\sigma_w^2(1+c)^2(1+c-c\rho^2)}{(1-\rho^2)(1+c-c\rho)(1+c+c\rho)(1+c+c\rho^2)} \end{aligned}$$

and  $\hat{J}_{\min} = \hat{J}(1/\alpha) = \sigma_w^2$ , where the scalar  $r \in [1, 3]$  is given by  $r := (1+c)(1-c+c\rho)/((1-c)(1+c-c\rho))$  and the scalar  $c \in [0, 1/2]$  is given by Proposition 4.

*Proof:* The values of  $h$ ,  $d$ , and  $l$  in (29) are given by

$$\begin{aligned} h(m) &= (1-c-c\rho^2)/(1-c) & h(L) &= (1+c+c\rho^2)/(1+c) \\ d(m) &= (1-\rho)(1-c-c\rho)/(1-c) & d(L) &= (1+\rho)(1+c-c\rho)/(1+c) \\ l(m) &= (1+\rho)(1-c+c\rho)/(1-c) & l(L) &= (1-\rho)(1+c+c\rho)/(1+c) \end{aligned} \quad (65a)$$

and the condition number is determined by

$$\kappa = \frac{\alpha L}{\alpha m} = \frac{d(L)}{d(m)} = \frac{l(m)}{rd(m)} \quad (65b)$$

where we let  $r := l(m)/d(L)$ . By combining this identity with the expressions in (65a), and rearranging terms, we can obtain the desired quadratic equation for  $c$  in terms of  $\rho$  and  $\kappa$ . To see that  $r \in [1, 3]$ , from Figure 3 we observe that as we change the orientation from gradient descent ( $c = 0$ ) to Nesterov's method with parameters that optimize the convergence rate ( $c = 1/2$ ),  $l(m)$  and  $1/d(L)$  monotonically increase. Thus,  $r$  is also increasing in  $c$ , and its smallest and largest values are obtained for  $c = 0$  and  $c = 1/2$ , respectively, which yields  $1 \leq r \leq 3(1+\rho)/(3-\rho) \leq 3$ .

As we demonstrate in Appendix B,  $\hat{J}$  as a function of  $(b, a)$  takes its minimum  $\hat{J}_{\min} = \sigma_w^2$  at the origin. In addition, for each  $c \in [0, 1/2]$ , the line segment  $(b(\lambda), a(\lambda))$ ,  $\lambda \in [m, L]$ , passes through the origin at  $\lambda = 1/\alpha$ . Thus, the minimum of  $\hat{J}(\lambda)$  occurs at  $\lambda = 1/\alpha$  and is given by  $\hat{J}_{\min} = \sigma_w^2$ .

We next show that  $\hat{J}(m)$  is the largest value of  $\hat{J}(\lambda)$  over  $[m, L]$ . Since  $\hat{J}(\lambda)$  is a convex function of  $\lambda$  (see Appendix B), it attains its maximum at one of the boundary points  $\lambda = m$  and  $\lambda = L$ . To show  $\hat{J}(m) > \hat{J}(L)$ , we first obtain expressions for  $\hat{J}(m)$  and  $\hat{J}(L)$  in terms of  $\rho$  and  $c$  by combining (65a) with the analytical expression for  $\hat{J}$  in Theorem 5. By properly rearranging terms and simplifying fractions, we can obtain the equivalence

$$\hat{J}(m) \geq \hat{J}(L) \iff c^4\rho^4 - c^4\rho^2 - c^2\rho^2 - c^2 + 1 \geq 0.$$

For  $\rho \in [0, 1]$  and  $c \in [0, 1/2]$ , it is easy to verify that the inequality on the right-hand holds.

To obtain the maximum value, we use Theorem 5 to write

$$\frac{\hat{J}(m)}{\sigma_w^2} = \frac{d(m) + l(m)}{2h(m)d(m)l(m)} = \frac{r\kappa + 1}{2h(m)l(m)} \quad (65c)$$

Combining (65a) with (65c) yields the desired value for  $\hat{J}(m)$ .  $\blacksquare$

Lemma 6 allows us to derive analytical expressions for the largest and smallest values that  $J$  takes over  $f \in \mathcal{Q}_m^L$ .

*Corollary 3:* The parameterized family of Nesterov-like methods (38) satisfies

$$\begin{aligned} J_{\max} &= (n-1)\hat{J}(m) + \hat{J}(L) \\ J_{\min} &= \hat{J}(m) + \hat{J}(L) + (n-2)\hat{J}(1/\alpha) \end{aligned}$$

where  $\hat{J}(m)$ ,  $\hat{J}(L)$ ,  $\hat{J}(1/\alpha)$  are given by Lemma 6, and  $J_{\max}$ ,  $J_{\min}$  are the extreme values of  $J$  when the algorithm is applied to  $f \in \mathcal{Q}_m^L$  with condition number  $\kappa = L/m$ .

*Proof:* The result follows from combining Lemma 6 and the expression  $J = \sum_{i=1}^n \hat{J}(\lambda_i)$  established in Theorem 5. In particular,  $J$  is maximized when  $Q$  has  $n-1$  eigenvalues at  $m$  and one at  $L$ , and it is minimized when, apart from the extreme eigenvalues  $m$  and  $L$ , the rest are at  $\lambda = 1/\alpha$ .  $\blacksquare$

We next establish order-wise tight upper and lower bounds on  $\hat{J}_{\max}/(1-\rho)$  and  $\hat{J}_{\min}/(1-\rho)$  in terms of  $\kappa$ .

*Lemma 7:* For the parameterized family of Nesterov-like methods (38), the largest and smallest modal contributions

to variance amplification established in Lemma 6 satisfy

$$\begin{aligned}\sigma_w^2 \omega_1 r \kappa (r \kappa + 1) &\leq \hat{J}_{\max} \times T_s \leq \sigma_w^2 \omega_2 r \kappa (r \kappa + 1) \\ \sigma_w^2 \sqrt{3\kappa + 1}/2 &\leq \hat{J}_{\min} \times T_s \leq \sigma_w^2 (\kappa + 1)/2\end{aligned}$$

where the scalar  $\omega_1 := (1+\rho)^{-3}(1-c)^2(1-c+c\rho)^{-2}/2$ ,  $\omega_2 := (1+\rho)\omega_1$ , and we have  $(1+\rho)^{-5} \leq \omega_1 \leq (1+\rho)^{-3}$ .

*Proof:* To obtain the upper and lower bounds on  $\hat{J}_{\max} \times T_s = \hat{J}(m) \times T_s$ , we combine (65b) and (65c) to write

$$\hat{J}(m) = \frac{r\kappa(r\kappa + 1)}{2h(m)(l(m))^2/d(m)}$$

where we set  $\sigma_w = 1$ . This equation in conjunction with the trivial inequalities

$$1 \leq (1 - \rho)h(m)/d(m) \leq 1 + \rho$$

allows us to write

$$\frac{r\kappa(r\kappa + 1)}{2(1 + \rho)l^2(m)} \leq \frac{\hat{J}(m)}{1 - \rho} \leq \frac{r\kappa(r\kappa + 1)}{2l^2(m)}. \quad (66)$$

Combining (65a) and (66) yields the desired bounds on  $\hat{J}_{\max}/(1-\rho)$ . Finally, the bounds on  $\hat{J}_{\min} \times T_s = \sigma_w^2/(1-\rho)$  can be obtained by noting that  $T_s = 1/(1-\rho) \in [\sqrt{3\kappa+1}/2, (\kappa+1)/2]$  as shown in Lemma 6.  $\blacksquare$

Similar to the heavy-ball-like methods,  $\hat{J}_{\max} \times T_s = \Theta(\kappa^2)$ . However, the upper and lower bounds on  $\hat{J}_{\min} \times T_s$  scale linearly with  $\kappa$  and  $\sqrt{\kappa}$ , respectively. We next use this result to bound  $J \times T_s$  and complete the proof of Proposition 4. In particular, we have

$$\begin{aligned}\sigma_w^2 ((n-1)\omega_1 r \kappa (r \kappa + 1) + \sqrt{3\kappa + 1}/2) &\leq J_{\max} \times T_s \leq \sigma_w^2 n \omega_2 r \kappa (r \kappa + 1) \\ \sigma_w^2 (\omega_1 r \kappa (r \kappa + 1) + (n-1)\sqrt{3\kappa + 1}/2) &\leq J_{\min} \times T_s \leq \sigma_w^2 (\omega_2 r \kappa (r \kappa + 1) + (n-1)(\kappa + 1)/2)\end{aligned}$$

where the scalar  $r \in [1, 3]$ , and  $\omega_1$  and  $\omega_2$  are given by Lemmas 6 and 7, respectively. To see this, note that as shown in the proof of Corollary 3,  $J/(1-\rho)$  is maximized when  $Q$  has  $n-1$  eigenvalues at  $m$  and one at  $L$ , and is minimized when, apart from the extreme eigenvalues  $m$  and  $L$ , the rest are placed at  $\lambda = 1/\alpha$ . Employing the bounds on  $\hat{J}_{\max} = \hat{J}(m)$  and  $\hat{J}_{\min} = \hat{J}(1/\alpha)$  provided by Lemma 7 and noting that  $\hat{J}(L) \in [\hat{J}_{\min}, \hat{J}_{\max}]$  completes the proof.

## E. Proofs of Section VI

1) *Proof of Lemma 5:* Stability can be verified using the Routh-Hurwitz criterion applied to the characteristic polynomial  $F(s) = \det(sI - M) = s^2 + bs + a$ . Similarly, conditions for  $\rho$ -exponential stability can be obtained by applying the Routh-Hurwitz criterion to the characteristic polynomial  $F_\rho(s)$  associated with the matrix  $M + \rho I$ , i.e.,

$$F_\rho(s) = s^2 + (b - 2\rho)s + \rho^2 - \rho b + a$$

and noting that strict inequalities become non-strict as we require  $\Re(\text{eig}(M + \rho I))$  to be non-positive.

2) *Proof of Proposition 5:* The  $\rho$ -exponential stability of (41b) with  $\alpha = 1/L$  is equivalent to the inclusion of the line segment  $(b(\lambda), a(\lambda))$ ,  $\lambda \in [m, L]$ , in the triangle  $\Delta_\rho$  in (44), where  $a(\lambda)$  and  $b(\lambda)$  are given by (42c). In addition, using the convexity of  $\Delta_\rho$ , this condition further reduces to the end points  $(b(L), a(L))$  and  $(b(m), a(m))$  belonging to  $\Delta_\rho$ . Now since  $a(L) = 1$ ,  $a(m) = 1/\kappa$ , the above condition implies

$$a_{\max}/a_{\min} \geq \kappa \quad (67)$$

where  $a_{\max}$  and  $a_{\min}$  are the largest and smallest values that  $a$  can take among all  $(b, a) \in \Delta_\rho$ . It is now easy to verify that  $a_{\max} = 1$  and  $a_{\min} = \rho^2$  correspond to the edge  $Y_\rho Z_\rho$  and the vertex  $X_\rho$  of  $\Delta_\rho$ , respectively; see Figure 5. Thus, inequality (67) yields the upper bound  $\rho \leq 1/\sqrt{\kappa}$  and we can achieve this rate with,

$$(b(m), a(m)) = X_\rho, (b(L), a(L)) = E_v \quad (68)$$

where  $E_v := (b_v, 1) = (2\rho + v(\rho - 1/\rho), 1)$ ,  $v \in [0, 1]$ , parameterizes the edge  $Y_\rho Z_\rho$ . Solving the equations in (68) for  $\gamma$  and  $\beta$  yields the optimal values of parameters. Finally, letting  $\gamma = 0$  and  $\gamma = \beta$  yields the conditions on  $v$  for the heavy-ball and Nesterov's method, respectively. The condition  $\kappa \geq 4$  for Nesterov's method stems from the fact that, for  $\alpha = 1/L$ , setting  $\gamma = \beta$  yields  $b(L) = 1$ . Thus, we have the necessary condition  $2\rho \leq 1$  to ensure  $(b(L), a(L)) \in \Delta_\rho$ ; see Figure 6. This completes the proof.

3) *Proof of Theorem 7:* Let  $G := (b_G, a_G)$  be the point on the edge  $X_\rho Z_\rho$  of the triangle  $\Delta_\rho$  in (44) such that

$$a_G = a(m), \quad b_G = a(m)/\rho + \rho.$$

Using  $(b(m), a(m)) \in \Delta_\rho$ , it is easy to verify that  $b_G \geq b(m)$ . This allows us to write

$$\frac{\hat{J}(m)}{\rho} = \frac{1}{2a(m)b(m)\rho} \geq \frac{1}{2a(m)b_G\rho} = \frac{1}{2a(m)(a(m) + \rho^2)}.$$

Combining the above inequality with  $a(m) = 1/\kappa$  and the upper bound  $\rho \leq 1/\sqrt{\kappa}$  from Lemma 5 yields

$$\hat{J}(m)/\rho \geq \kappa^2/4. \quad (69)$$

Noting that among the points in  $\Delta_\rho$ , the modal contribution  $\hat{J} = 1/(2ab)$  takes its minimum value

$$\hat{J}_{\min} = 1/(2\rho + 2/\rho) \quad (70)$$

at the vertex  $Z_\rho = (1, \rho + 1/\rho)$ , we can write

$$\frac{J}{\rho} = \frac{\hat{J}(m)}{\rho} + \sum_{i=1}^{n-1} \frac{\hat{J}(\lambda_i)}{\rho} \geq \frac{\kappa^2}{4} + \frac{n-1}{2(1+\rho^2)}$$

where we use (69) to lower bound the first term  $\hat{J}(m)/\rho$ . This completes the proof of (48b).

To prove the lower bound in (48a), we consider a quadratic objective function for which the Hessian has  $n-1$  eigenvalues at  $\lambda = m$  and one eigenvalue at  $\lambda = L$ . For such a function, we can write

$$J_{\max} \geq J = \hat{J}(m)(n-1) + \hat{J}(L).$$

Finally, we lower bound the right hand-side using (69) and (70) to complete the proof.

#### F. Lyapunov equations and the steady-state variance

For discrete-time LTI system (4a), the covariance matrix  $P^t := \mathbb{E}(\psi^t(\psi^t)^T)$  of the state vector  $\psi^t$  satisfies the linear recursion

$$P^{t+1} = AP^tA^T + BB^T \quad (71a)$$

and its steady-state limit

$$P := \lim_{t \rightarrow \infty} \mathbb{E}[\psi^t(\psi^t)^T] \quad (71b)$$

is the unique solution to the algebraic Lyapunov equation [42],

$$P = APA^T + BB^T. \quad (71c)$$

For stable LTI systems, performance measure (8) can be computed using

$$J = \lim_{t \rightarrow \infty} \frac{1}{t} \sum_{k=0}^t \text{trace}(Z^k) = \text{trace}(Z) \quad (71d)$$

where  $Z = CPC^T$  is the steady-state limit of the output covariance matrix  $Z^t := \mathbb{E}[z^t(z^t)^T] = CP^tC^T$ . We can prove Theorem 5 by finding the solution  $P$  to (71c) for the two-step momentum algorithm.

The above results carry over to the continuous-time case with the only difference that the Lyapunov equation for the steady-state covariance matrix of  $\psi(t)$  is given by  $AP + PA^T = -BB^T$ .

#### REFERENCES

- [1] B. T. Polyak, "Some methods of speeding up the convergence of iteration methods," *USSR Comput. Math. & Math. Phys.*, vol. 4, no. 5, pp. 1–17, 1964.
- [2] Y. Nesterov, "A method for solving the convex programming problem with convergence rate  $O(1/k^2)$ ," in *Dokl. Akad. Nauk SSSR*, vol. 27, 1983, pp. 543–547.
- [3] Y. Nesterov, "Gradient methods for minimizing composite objective functions," *Math. Program.*, vol. 140, no. 1, pp. 125–161, 2013.
- [4] L. Bottou and Y. Le Cun, "On-line learning for very large data sets," *Appl. Stoch. Models Bus. Ind.*, vol. 21, no. 2, pp. 137–151, 2005.
- [5] A. Beck and M. Teboulle, "A fast iterative shrinkage-thresholding algorithm for linear inverse problems," *SIAM J. Imaging Sci.*, vol. 2, no. 1, pp. 183–202, 2009.
- [6] M. Hong, M. Razaviyayn, Z.-Q. Luo, and J.-S. Pang, "A unified algorithmic framework for block-structured optimization involving big data: With applications in machine learning and signal processing," *IEEE Signal Process. Mag.*, vol. 33, no. 1, pp. 57–77, 2016.

- [7] A. Badithela and P. Seiler, "Analysis of the heavy-ball algorithm using integral quadratic constraints," in *Proceedings of the 2019 American Control Conference*. IEEE, 2019, pp. 4081–4085.
- [8] I. Sutskever, J. Martens, G. Dahl, and G. Hinton, "On the importance of initialization and momentum in deep learning," in *Proc. ICML*, 2013, pp. 1139–1147.
- [9] Y. Nesterov, *Lectures on convex optimization*. Springer Optimization and Its Applications, 2018, vol. 137.
- [10] L. Lessard, B. Recht, and A. Packard, "Analysis and design of optimization algorithms via integral quadratic constraints," *SIAM J. Optim.*, vol. 26, no. 1, pp. 57–95, 2016.
- [11] B. Hu and L. Lessard, "Dissipativity theory for Nesterov's accelerated method," in *Proceedings of the 34th International Conference on Machine Learning*, ser. Proc. Mach. Learn. Res., 2017, pp. 1549–1557.
- [12] S. Cyrus, B. Hu, B. Van Scoy, and L. Lessard, "A robust accelerated optimization algorithm for strongly convex functions," in *Proceedings of the 2018 American Control Conference*, 2018, pp. 1376–1381.
- [13] B. V. Scoy, R. A. Freeman, and K. M. Lynch, "The fastest known globally convergent first-order method for minimizing strongly convex functions," *IEEE Control Syst. Lett.*, vol. 2, no. 1, pp. 49–54, 2018.
- [14] M. Fazlyab, A. Ribeiro, M. Morari, and V. M. Preciado, "Analysis of optimization algorithms via integral quadratic constraints: Nonstrongly convex problems," *SIAM J. Optim.*, vol. 28, no. 3, pp. 2654–2689, 2018.
- [15] B. T. Polyak, "Comparison of the convergence rates for single-step and multi-step optimization algorithms in the presence of noise," *Engrg.Cybern.*, vol. 15, no. 1, pp. 6–10, 1977.
- [16] Y. Bengio, "Gradient-based optimization of hyperparameters," *Neural Comput.*, vol. 12, no. 8, pp. 1889–1900, 2000.
- [17] D. Maclaurin, D. Duvenaud, and R. Adams, "Gradient-based hyperparameter optimization through reversible learning," in *Proc. ICML*, 2015, pp. 2113–2122.
- [18] K. Yuan, B. Ying, and A. H. Sayed, "On the influence of momentum acceleration on online learning," *J. Mach. Learn. Res.*, vol. 17, no. 1, pp. 6602–6667, 2016.
- [19] A. Beirami, M. Razaviyayn, S. Shahrampour, and V. Tarokh, "On optimal generalizability in parametric learning," in *Proc. Neural Information Processing (NIPS)*, 2017, pp. 3458–3468.
- [20] Z.-Q. Luo and P. Tseng, "Error bounds and convergence analysis of feasible descent methods: a general approach," *Ann. Oper. Res.*, vol. 46, no. 1, pp. 157–178, 1993.
- [21] H. Robbins and S. Monro, "A stochastic approximation method," *Ann. Math. Statist.*, pp. 400–407, 1951.
- [22] A. Nemirovski, A. Juditsky, G. Lan, and A. Shapiro, "Robust stochastic approximation approach to stochastic programming," *SIAM J. Optim.*, vol. 19, no. 4, pp. 1574–1609, 2009.
- [23] O. Devolder, "Exactness, inexactness and stochasticity in first-order methods for large-scale convex optimization," Ph.D. dissertation, Louvain-la-Neuve, 2013.
- [24] P. Dvurechensky and A. Gasnikov, "Stochastic intermediate gradient method for convex problems with stochastic inexact oracle," *J. Optimiz. Theory App.*, vol. 171, no. 1, pp. 121–145, 2016.
- [25] B. O'Donoghue and E. Candes, "Adaptive restart for accelerated gradient schemes," *Found. Comput. Math.*, vol. 15, pp. 715–732, 2015.
- [26] B. T. Polyak and G. V. Smirnov, "Transient response in matrix discrete-time linear systems," *Autom. Remote Control*, vol. 80, no. 9, pp. 1645–1652, 2019.
- [27] H. Mohammadi, S. Samuelson, and M. R. Jovanović, "Transient growth of accelerated optimization algorithms," *IEEE Trans. Automat. Control*, 2022, doi:10.1109/TAC.2022.3162154.
- [28] O. Devolder, "Stochastic first order methods in smooth convex optimization," Catholic Univ. Louvain, Louvain-la-Neuve, Tech. Rep., 2011.
- [29] M. B. Cohen, J. Diakonikolas, and L. Orecchia, "On acceleration with noise-corrupted gradients," in *Proceedings of the 35th International Conference on Machine Learning*, ser. Proc. Mach. Learn. Res., vol. 80, 2018, pp. 1019–1028.
- [30] H. Mohammadi, M. Razaviyayn, and M. R. Jovanović, "Robustness of accelerated first-order algorithms for strongly convex optimization problems," *IEEE Trans. Automat. Control*, vol. 66, no. 6, pp. 2480–2495, 2021.
- [31] B. V. Scoy and L. Lessard, "The speed-robustness trade-off for first-order methods with additive gradient noise," 2021, arXiv:2109.05059.
- [32] N. S. Aybat, A. Fallah, M. M. Gürbüzbalaban, and A. Ozdaglar, "Robust accelerated gradient methods for smooth strongly convex functions," *SIAM J. Opt.*, vol. 30, no. 1, pp. 717–751, 2020.
- [33] Y. Nesterov, *Introductory lectures on convex optimization: A basic course*. Springer Science & Business Media, 2004, vol. 87.
- [34] Y. Arjevani, S. Shalev-Shwartz, and O. Shamir, "On lower and upper bounds in smooth and strongly convex optimization," *J. Mach. Learn. Res.*, vol. 17, no. 1, pp. 4303–4353, 2016.
- [35] M. Muehlebach and M. Jordan, "A dynamical systems perspective on Nesterov acceleration," in *International Conference on Machine Learning*. PMLR, 2019, pp. 4656–4662.
- [36] Z. He, A. S. Rakin, and D. Fan, "Parametric noise injection: Trainable randomness to improve deep neural network robustness against adversarial attack," in *Proceedings of the IEEE/CVF Conference on Computer Vision and Pattern Recognition*, 2019, pp. 588–597.
- [37] B. T. Polyak, "Introduction to optimization," *Optimization Software Inc., New York*, vol. 1, 1987.
- [38] R. Bassily, A. Smith, and A. Thakurta, "Private empirical risk minimization: Efficient algorithms and tight error bounds," in *2014 IEEE 55th Annual Symposium on Foundations of Computer Science*, 2014, pp. 464–473.
- [39] S. B. Gelfand and S. K. Mitter, "Recursive stochastic algorithms for global optimization in  $R^d$ ," *SIAM J. Control Optim.*, vol. 29, no. 5, pp. 999–1018, 1991.
- [40] M. Raginsky, A. Rakhlin, and M. Telgarsky, "Non-convex learning via stochastic gradient Langevin dynamics: a nonasymptotic analysis," in *Proceedings of the Conference on Learning Theory*, ser. Proc. Mach. Learn. Res., vol. 65, 2017, pp. 1674–1703.
- [41] Y. Zhang, P. Liang, and M. Charikar, "A hitting time analysis of stochastic gradient Langevin dynamics," in *Proceedings of the 2017 Conference on Learning Theory*, ser. Proc. Mach. Learn. Res., vol. 65, 2017, pp. 1980–2022.
- [42] H. Kwakernaak and R. Sivan, *Linear optimal control systems*. Wiley-Interscience, 1972.
- [43] K. Ogata, *Discrete-time control systems*. New Jersey: Prentice-Hall, 1994.
- [44] R. Padmanabhan and P. Seiler, "Analysis of gradient descent with varying step sizes using integral quadratic constraints," 2022, arXiv:2210.00644.
- [45] B. Hu, P. Seiler, and A. Rantzer, "A unified analysis of stochastic optimization methods using jump system theory and quadratic constraints," in *Proceedings of the 2017 Conference on Learning Theory*, ser. Proc. Mach. Learn. Res., 2017, pp. 1157–1189.
- [46] B. Hu, P. Seiler, and L. Lessard, "Analysis of biased stochastic gradient descent using sequential semidefinite programs," *Math. Program.*, vol. 187, no. 1, pp. 383–408, 2021.